

# Joint scaling laws in functional and evolutionary categories in prokaryotic genomes.

J. Grilli<sup>1</sup>, B. Bassetti<sup>1,2</sup>, Sergei Maslov<sup>3</sup>, M. Cosentino Lagomarsino<sup>4,5,\*</sup>

**1** Dipartimento di Fisica, Università degli Studi di Milano, Milano, Italy

**2** I.N.F.N. Milano, Milano, Italy

**3** Department of Condensed Matter Physics and Materials Science, Brookhaven National Laboratory, Upton, NY 11973, United States of America

**4** Génophysique / Genomic Physics Group, UMR 7238 CNRS “Microorganism Genomics”, Paris, France

**5** Université Pierre et Marie Curie, Paris, France

\* E-mail: Marco.Cosentino-Lagomarsino@upmc.fr

## Abstract

We propose and study a class-expansion/innovation/loss model of genome evolution taking into account biological roles of genes and their constituent domains. In our model numbers of genes in different functional categories are coupled to each other. For example, an increase in the number of metabolic enzymes in a genome is usually accompanied by addition of new transcription factors regulating these enzymes. Such coupling can be thought of as a proportional “recipe” for genome composition of the type “a spoonful of sugar for each egg yolk”. The model jointly reproduces two known empirical laws: the distribution of family sizes and the nonlinear scaling of the number of genes in certain functional categories (e.g. transcription factors) with genome size. In addition, it allows us to derive a novel relation between the exponents characterizing these two scaling laws, establishing a direct quantitative connection between evolutionary and functional categories. It predicts that functional categories that grow faster-than-linearly with genome size to be characterized by flatter-than-average family size distributions. This relation is confirmed by our bioinformatics analysis of prokaryotic genomes. This proves that the joint quantitative trends of functional and evolutionary classes can be understood in terms of evolutionary growth with proportional recipes.

## 1 Introduction

Protein-coding genes in genomes can be classified in both functional categories (e.g. transcription factors or metabolic enzymes) as well as “evolutionary categories” or families of homologous genes (to avoid confusion, in the following we will reserve the term “category” to functional annotations, and we will use the term “family” as a generic indication of homology classes, or domain families/superfamilies in domain data, see Methods). Functional categories are routinely composed of a large number of evolutionary ones. This distinction is illustrated in Fig. 1, where genes are characterized by both shape (functional category) and color (homology class) with each shape represented by multiple colors. Understanding the principles connecting these separate classifications of genomic material is an important step in order to disentangle the organization of the content of whole genomes.

More specifically, studies of fully sequenced genomes revealed that their functional and evolutionary composition is governed by simple quantitative laws [1, 2]. In particular, for prokaryotes the number of genes in individual functional categories was shown to scale as a power law of the total number of genes in the genome [2]. Depending on the functional category the exponent of this scaling law varies from 0 (for fixed sets of housekeeping genes) to 1 (for metabolic enzymes) and all the way up to 2 (for transcription factors and kinases) [2, 3]. Furthermore, the distribution of sizes of gene families (called “evolutionary categories” in our title) has a scale-free distribution with the exponent inversely correlated with the genome size [1, 4, 5]. The overall number of gene (or domain) families represented by at least one member

exhibits a slower-than-linear scaling with the total number of genes in a genome [6, 7]. Biologically, the growth of evolutionary families derives from combined processes of horizontal gene transfer, gene duplication, gene genesis, and gene loss [8]. For prokaryotes, horizontal transfer appears to dominate gene family expansion [9], and the same process is presumably very important for the introduction of a new evolutionary family into an extant genome.

The comprehension of these empirical laws requires to construct quantitative models that explore different design principles, or more prosaically the recipes by which genomes are built from elementary functional and evolutionary ingredients. In this study we introduce the first model to jointly explain observed scaling laws for evolutionary families and functional categories.

Several theoretical models have been previously proposed to explain the observed power-law distribution of family sizes [5, 10–13]. Most of these models are of class-expansion/innovation/loss type, abstractly mimicking basic evolutionary moves such as horizontal transfer, duplication, loss. We recently formulated a related model that in addition to family size distribution also explains and successfully fits the scaling of the number of distinct gene families represented in a genome as a function of genome size [6, 14].

On another front, the “toolbox model” of evolution of metabolic networks and their regulation recently proposed by one of us [15] offered an explanation for the quadratic scaling between the number of transcription factors and the total number of genes in prokaryotes. In this model, metabolic and regulatory networks of prokaryotes are shaped by addition of co-regulated metabolic pathways. The number of added enzymes systematically decreases with the proportion to which the organism has already explored the universe of available metabolic reactions, and thus, indirectly, with the size of its genome. For the purposes of the present study, a key ingredient of the toolbox model is that events adding or deleting genes in multiple functional categories (in this case metabolic enzymes and transcription factors regulating metabolic pathways) are tightly correlated with each other. The concept of coordinated expansion or contraction of functional categories can in principle be extended beyond enzymes and their regulators.

One should note that this explanation of scaling of functional categories is conceptually different from that based on “evolutionary potentials” proposed in Ref. [3]. Evolutionary potentials quantify the intrinsic growth rates of individual categories. This means that in this model the growth of one functional category is represented as uncoupled from growth or decline in other functional categories. However, evolutionary potentials could also be the effective result of the coordinated expansion of multiple functional categories linked by interactions of biological and evolutionary origin (e.g. linking membrane proteins with signal transduction, etc.) On the other hand, it is clear that models with evolutionary potentials represent quite well the empirical data on the growth of functional categories, and thus it appears that this must be (at least) a very good effective description, that any more detailed model needs to reproduce.

This study brings together the basic ingredients of class-expansion/innovation/loss models [6, 14] and coordinated growth of functional categories [15]. The resulting combination allows us to study the interplay between the scaling of evolutionary and functional categories. In particular, we mathematically derive a relation between the exponents characterizing these two scaling laws. It predicts that functional categories that grow faster-than-linearly with genome size are characterized by flatter-than-average family size distributions. This prediction of our model is subsequently verified by our analysis of functional and evolutionary scaling in empirical data on sequenced prokaryotic genomes. Finally, we analyze and discuss the alternative combination of a class-expansion/innovation/loss model with growth of functional categories dictated by evolutionary potentials.

## 2 MATERIALS AND METHODS

### Models

The model represents a genome as a list of genes, which is partitioned in homology families and functional categories. Genome evolution is modeled as a stochastic process where the elementary moves can be

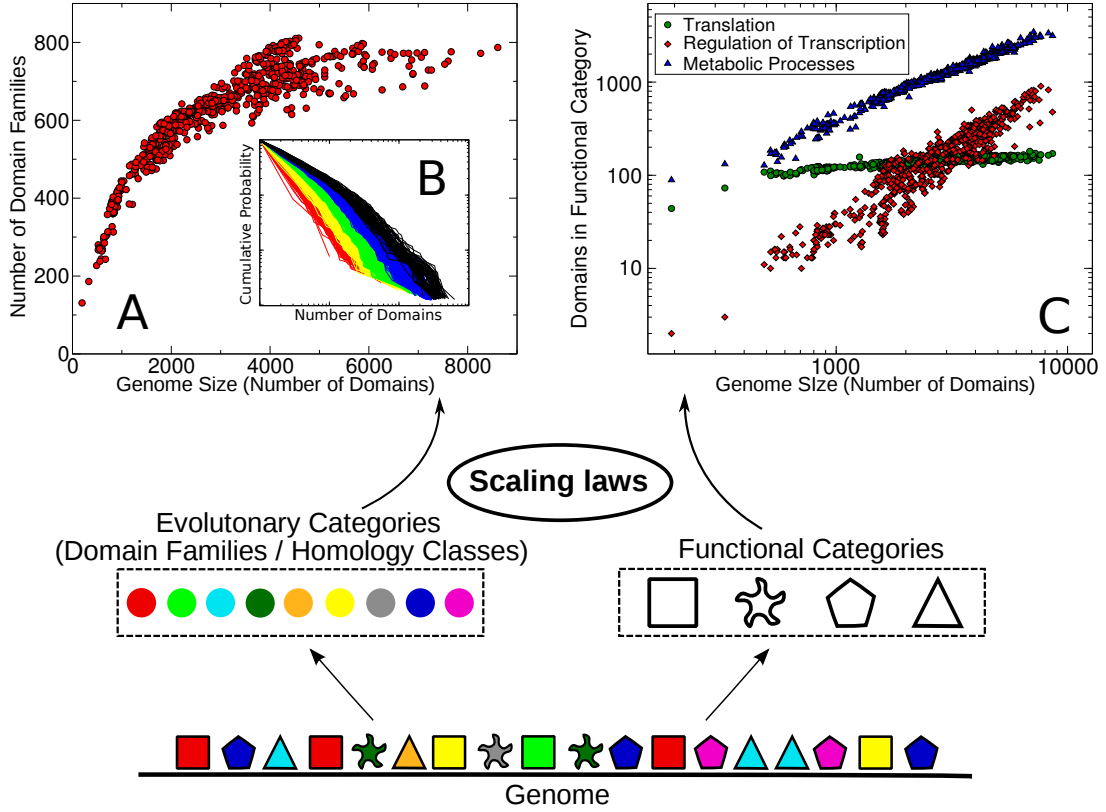


**Figure 1.** Scaling laws in joint functional/evolutionary partitioning of genomes. Genomes are partitioned into families of homologous genes (colors) and functional categories (shapes). (A) The number of unique evolutionary categories (domain families) (y-axis) scales sub-linearly with the genome size (x-axis.) (B) Cumulative histograms of domain family size (see Figure 4). (C) The number of transcriptional regulators (red), metabolic enzymes (blue), and housekeeping genes responsible for translation (green) plotted as a function of the genome size measured by the total number of domains. Symbols in all the plots are empirical data for protein domains in 753 fully sequenced bacterial genomes.

any of two types: (i) a “family expansion” or “duplication” move in which a new domain is placed in an evolutionary category (family of homologous domains) already present in the genome or (ii) an “innovation” move in which a new family with just one domain appears in a genome (e.g. by the virtue of horizontal gene transfer).

We would like to emphasize that in the tradition established in “duplication-innovation-loss” models, which we follow, the family expansion move is customarily labeled as duplication. In reality this move can come either by the virtue of gene duplication or by horizontal gene transfer, which appears to be the dominant class-expansion mechanism in bacteria [9]. The overall family size in all genomes might be generating an effective “preferential attachment” for HGT events (see Refs. [3, 16] and open comments by referees therein).

Although genes are natural objects of this kind of description, it is not simple to use genes as central units in the analysis of empirical data, mainly due to the fact that gene dynamics is complex and may contain events of gene fusion, splitting and internal rearrangements. Thus, as in some previous analyses, we will compare the models with data on protein domains [3, 6], which have the important property that

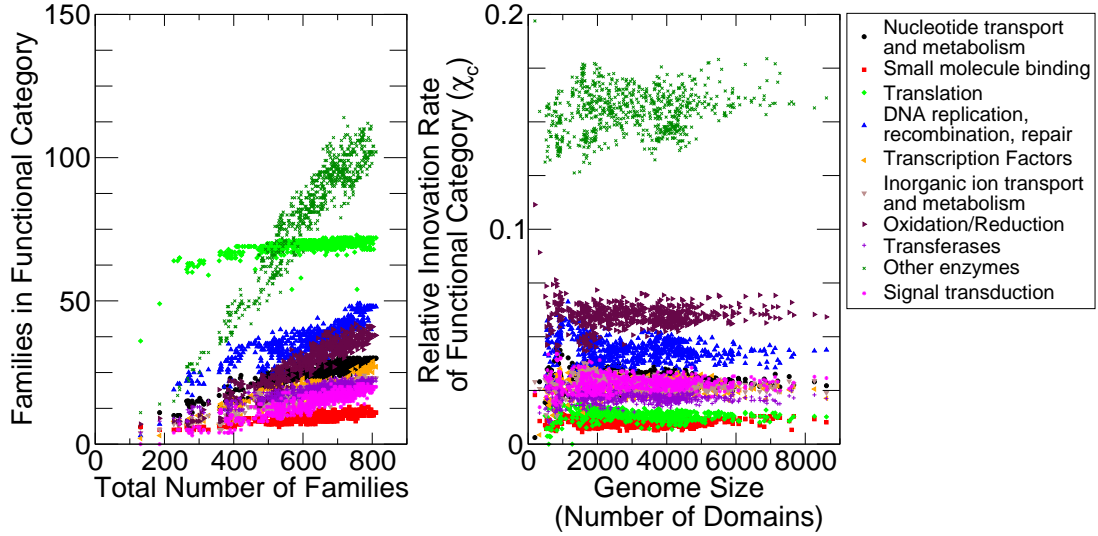


**Figure 2.** The number of evolutionary (domain) families belonging to a functional category follows a linear law in empirical data, denoting a possible invariant of genome composition. The left panel plots the data on for the number of families  $f_c$  in the ten largest functional categories on all genomes, following the trend  $f_c = A_c + \chi_c f$ , where  $f$  is the total number of families on the genome. Symbols are empirical data for 753 fully sequenced bacterial genomes. The offset  $A_c$  is large only for the “translation” category. The right panel is a plot of the coefficients  $\chi_c$  obtained from the same data (subtracting the offset  $A_c$  obtained from a linear fit), as a function of genome size in domains,  $n$ . See also Supplementary Table S1.

they cannot be split into smaller units [17]. Domains are modular building blocks of proteins and it has been argued that they effectively work as the natural atomic elements in genome evolution [4]. Concerning the scaling laws, domains appear to have the same qualitative behaviour as genes. Throughout the paper, we will be comparing the models with data on 753 bacteria from the SUPERFAMILY database [18]. The models will be formulated for abstract atomic elements that could be genes or domains, and possible relevant issues when dealing empirically with genes will be addressed in the discussion. In describing the models we will generally refer to these units as genes.

Technically, in order to compare with the protein domain data we rely on simplifying assumptions on the domain composition of proteins. Obviously the situation is more complex than this. We have verified in the data that the number of TF domains are linear in the number of TF genes (Supplementary Figure S5), with slope 1.09 (average number of TF domains in a TF gene). A second assumption is that the number of families belonging to a functional category is linear in the total number of families. This assumption is in accordance with data (see Figure 2 and Supplementary Figure S1). In particular, we observed this trend for the number of transcription factor superfamilies (see Supplementary Figure S2).

### Standard Chinese Restaurant Process.

The starting point is a class-expansion/innovation process for the homology families that reproduces qualitatively the empirical scaling laws [6]. This process (known in mathematical literature as “Chinese Restaurant Process” or CRP [19]) defines a growth dynamics for the partitioning of a set of elements (genes or domains) based on two basic growth moves. Traditionally the CRP model is defined by two parameters  $\alpha$  and  $\theta$  constrained by  $0 \leq \alpha \leq 1$  and  $\theta > -\alpha$ . The moves are quantified and defined by two

probabilities  $p_O$  and  $p_N$  of duplication and innovation respectively.

- The class-expansion probability  $p_O^i$  of a domain family  $i$  is proportional to the number of family members  $n_i$  currently in the genome offset by  $\alpha$ :  $p_O^i \sim n_i - \alpha$  (see Table 1).
- The innovation probability  $p_N$  is the probability of adding a new domain family with one member. It corresponds to a new domain family appearing in a genome by *de novo* evolution or horizontal gene transfer. The CRP model assumes  $p_N \sim \alpha f + \theta$ , where  $f$  is the total number of domain families present in the genome.

The normalization condition  $p_N + \sum_i p_O^i = 1$  determines the pre-factor in both equations to be  $1/(n + \theta)$ . A gene loss move does not seem to be essential for the basic qualitative results. Indeed, if stochastic (uniform) gene loss is incorporated into the model it results only in renormalization of parameters  $p_O$  and  $p_N$  [14].

We explore the model by direct simulation and by solving continuous “mean-field” equations [6, 14] that describe the mean behaviour of the number of homology families and functional categories, and the statistics of the population of families and categories.

### CRP model incorporating functional categories.

In order to introduce functional categories into the CRP, one has to specify  $p_O$  and  $p_N$  for different categories. We first assume that the probability of introducing a gene of a specific functional category by the innovation move is independent of genome size. This assumption implies that the number of homology families of a given category scales linearly in the total number of families, and is justified empirically for some functional categories by domain data (see Figure 2 and Supplementary Figures S1 and S2). Equivalently,  $p_N^c = \chi_c p_N$ , where  $\chi_c$  is the probability of introducing a new family of the category  $c$ . In other words, it is assumed here that every time a new family is added, the probability that it will belong to category  $c$  is  $\chi_c$ .

Under this assumption, the mean-field equation describing the growth of a family of homologous domains (evolutionary category) is

$$C(n)\partial_n n_i = \sum_{j=1}^f a_{ij} n_j - \alpha. \quad (1)$$

Here the genome size  $n$  is used instead of time and averages over multiple realizations of a process are implied. The novel ingredient of the model - coordinated growth of functional categories - is encoded in the coefficients  $a_{ij}$  responsible for correlated duplications between evolutionary families  $i$  and  $j$ . We assume  $a_{ij}$  to depend only on functional roles of families  $i$  and  $j$ . The equation describing the growth of  $f$  - the number of distinct families in a genome is the same as in a standard CRP model.

$$C(n)\partial_n f = (\alpha f + \theta). \quad (2)$$

The function  $C(n)$ , which sets a natural time scale for the process, is determined by the normalization condition  $\partial_n n = 1$ , i.e.  $\sum_i \partial_n n_i + \partial_n f = 1$ .

For the specific case of categories of transcription factors (TFs) regulating metabolic processes and their metabolic target enzymes, the necessity of a correlated move can be argued along the lines of Ref. [15]. A set of new targets has to be added to incorporate a new metabolic function. This entails the addition of a new metabolic pathway that is long enough to connect a new nutrient to a previously existing pathway, that further converts it to a central metabolic “core network”. Supposing that each newly added branch is controlled by only one added transcription factor, since the length of the branch becomes smaller with increasing size of the organismal metabolic network (compared to a metabolic

“universe”), on average, increasingly more TFs per target will be needed in order to control newly incorporated branches.

More generally, functional, genetic and epistatic interactions can create the correlated growth of different functional categories of genes. In the discussion section we provide the empirical evidence of statistically significant correlations between various functional categories.

Following the recipe outlined in Ref. [15] we consider a simplified version of the model involving only two functional categories: 1) *TF*- transcription factors controlling metabolic processes; 2) *met* - metabolic enzymes they regulated. As in the toolbox model, changes in  $n_{TF}$  and  $n_{met}$  are coordinated with correlation coefficients  $a_{ij}$  given by

$$a_{ij} = \frac{n_{met}}{U}, \quad a_{ji} = 0; \text{ for } i \neq j$$

$$\text{and } a_{ii} = 0.$$

Here  $U$  is the size of the metabolic universe,  $i$  denotes any gene family from functional category *TF*, and  $j$  - from the functional category *met*. In this variant, addition of transcription factors can only occur conditionally to the addition of metabolic enzymes. In the following, we will refer to this model variant as model Ia. We define a second variant of the correlated model (model Ib), which is a more direct extension of the standard CRP model, and thus can exploit previous mean-field theory analytical results. In this case

$$a_{ij} = \frac{n_i}{n_{met}}, \quad a_{ji} = 0; \text{ for } i \neq j$$

$$\text{and } a_{ii} = 1,$$

(where  $i$  again denotes any gene family from functional category *TF* and  $j$  - from the functional category *met*). In this model variant, all families (and hence also transcription factors families) have an equal intrinsic growth rate on top of the correlation. If  $a_{ij} = 0$ ,  $i \neq j$  the model is equivalent to the standard CRP. Finally, we also considered a model (model II) where correlations between functional categories are absent, but instead members of a given functional category are added at a category-dependent intrinsic rate as prescribed by “evolutionary potentials” of Molina and van Nimwegen (in this case,  $a_{ij} = 0$  for  $i \neq j$ , and  $a_{ii} = \rho_{c(i)}$ , where  $c(i)$  is the functional category to which family  $i$  belongs, and  $\rho_{c(i)}$  is the evolutionary potential of class  $c$ ). These results are discussed later on in the manuscript and compared to the two “correlated duplication” models above (see Discussion and Supplementary Text).

To resume, two kinds of models are considered here: “correlated recipes”, where the scaling exponents can only result from interactions between categories (model Ia and Ib, the main focus of our study), and “absolute recipes” (model II), leading to different intrinsic growth rates for different categories. Correlated models might contain an specific intrinsic growth rate of the classes, equal for all classes (model Ib), or not (model Ia). We will see that the important distinction between model I (a and b) and model II is that the different scaling exponents for functional categories are a result of correlations and not absolute class expansion rates.

## Data

Data on superfamily domain assignments and superfamily functional annotations for the 753 Bacteria were obtained from the SUPERFAMILY (v1.73) database [18]. The database contains 1291 different domain superfamilies grouped into 47 different functional categories (60 families do not belong to a specific category). These categories are divided into 6 larger groups (Metabolism, General, Regulation, Information, Initiation Complex Processes and Elongation Complex Processes, see also [http://supfam.cs.bris.ac.uk/SUPERFAMILY\\_1.73/function](http://supfam.cs.bris.ac.uk/SUPERFAMILY_1.73/function)).

## Evaluation of exponents in empirical data

We considered the normalized cumulative histograms (families with more than  $d$  members) and non-cumulative histograms (families with exactly  $d$  members) of the populations for all evolutionary families (related to exponent  $\beta$ , see Results), and those restricted to the families belonging to each of the main functional categories indexed by  $c$  (related to the exponent  $\beta_c$ , see Results). Exponents were estimated by fitting the data with a power-law, restricting to a window where the  $x$  axis value was less than a cutoff value, as in Ref. [14]. The cutoff was chosen for each fit, by minimizing the chi square residuals with varying window size. This procedure was implemented with a custom CINT (C++) script using the ROOT software. Figure 6 is obtained considering the fitted exponents for the histograms of the five largest genomes (where the “finite-size correction” is smallest, see Figure 5 and Ref. [14].)

## Empirical correlations among functional categories

Correlation between families (or categories) populations were calculated from the deviations from the average trend. We obtained the frequency of a family/category in every genome, defined as the ratio between the population of a family in domains and the total number of domains assigned on that genome. Subsequently for every family/category, we extracted an average trend as a function of genome size  $n$  using a sliding-window histogram (with window size of 280 domains and resolution of 28 domains), and we considered the deviation of each genome from the average trend at its value of  $n$ . The Pearson correlation of these deviations over all the genomes was considered between each pair of families/categories (Figure 7 and Supplementary Table S3 and S4).

## Models and simulations

The quantitative duplication-innovation evolutionary models were explored by a mean-field analytical approach and direct numerical simulations. The mean-field approach considers equations for the means of the observed quantities in the large- $n$  approximation. In parallel with the mean-field analysis, we performed simulations of the main model and its variants. The realizations depend on the following parameters. (i) The parameters of a standard CRP,  $\alpha$  and  $\theta$ . (ii) The parameter  $\chi_c$ , i.e. the probability that a new family belongs to a given functional category. This parameter can be inferred from data (see Results and Figure 2). For example, for the case of transcription factors and targets, we defined  $\chi_{TF}$  from the slope extrapolated from Supplementary Figure S2, giving  $\chi_{TF} \simeq 0.035$  (see also Supplementary Figure S6). (iii) Initial conditions, represented by initial configuration (number of leaves, number of TFs and number of families in both categories). We have used the configuration of the smallest bacterium in the dataset (*Candidatus Carsonella ruddii*). An alternative choice could be the minimal intersection of all genomes in the database. (iv) Variant-specific parameters, that amount to the evolutionary potentials  $\rho_c$  for the first variant of the model, and the correlation matrix between functional categories,  $a_{ij}$  for the second variant. Simulation results are typically visualized in boxplots in order to compare the means with the probability distributions. In these plots bars correspond to (in order) the smallest observation, lower quartile, median, upper quartile, and largest observation.

# 3 RESULTS

## A new invariant of genome composition

We found (Figure 2 and Supplementary Table See also Supplementary Table S1) that the number of evolutionary domain families forming a functional category follows a linear law in empirical data, denoting a possible invariant of genome composition. This also implies that the mean law  $\partial_n f_c = \chi_c \partial_n f$  assumed in the model is justified by the data. This does not mean exactly that the fraction of all families belonging

to a certain functional category is constant. Rather, the observed law can be  $f_c = A_c + \chi_c f$ , with an offset  $A_c$  representing a minimal amount of evolutionary families required to build a given functional category. In empirical data, this offset appears to be large only for the “translation” functional category.

## The model captures the combined scaling laws

Numerical simulation and mean-field analytical solutions of the correlated growth model (model I) reproduce very well both the empirical behavior of the TFs scaling law and the statistics for evolutionary domain families (Figure 3 and Supplementary Figure S4). We found no significant qualitative difference between models Ia and Ib regarding these observables. Furthermore, the joint scaling laws can be reproduced also with an uncorrelated model (model II), with minor technical difficulties (see Discussion). The correct asymptotic quadratic scaling can be obtained from mean-field arguments for both model I and II. These arguments are presented in the Supplementary Text. In order to illustrate this point we consider for example model Ib. Starting from Eqs. 1 one has to sum over all domain families from functional categories  $TF$  and  $met$ . Since  $n_{TF} = \sum_{i \in TF} n_i$ , depends on the number of TF classes, one must have for its derivative  $\partial_n n_{TF} = \sum_{i \in TF} \partial_n n_i + \partial_n f_{TF}$ . Combined, these two equations give  $dn_{TF}/dn_{met} = 2(n_{TF} - \alpha)/(n_{met} - \alpha) \simeq 2n_{TF}/n_{met}$ , or finally the quadratic scaling  $n_{TF} \sim n_{met}^2$ .

Altogether, the agreement between data and model is universal, in the sense that the same three parameters are sufficient to predict family/category numbers and populations for all genomes in the dataset. Moreover, the comparison does not rely on the adjustment of any hidden parameter. It is also worthwhile noting that, while the input of model I (a and b) is built to give an asymptotic power-law scaling exponent of two for transcription factors (which is reproduced by the mean-field approach), at the relevant genome sizes the model automatically reproduces the *correct* empirical exponent (about 1.6 in the SUPERFAMILY data) as an effect of the finite system size. Note that in model Ib TFs can duplicate both spontaneously (uncorrelated move) and following spontaneous duplication of targets (correlated move), corresponding to the terms  $a_{ii}$  and  $a_{ij}$  in equation 1, while in model Ia this does not happen.

The extension of the model to more than two categories requires to know the laws through which families of different categories are correlated with each other. Supplementary Figure S3 compares the results obtained by a correlated duplication model formulated with three categories (TFs, met, others).

**Table 1.** Basic model quantities and notations

Quantity	Meaning
$\alpha, \theta$	CRP model parameters
$n$	Genome size quantified by its total number of domains
$n_i$	Number of domains in the family $i$
$n_c$	Number of domains in the functional category $c$
$f(n)$	Number of families in a genome of size $n$
$f_c(n)$	Number of families in a genome of size $n$ belonging to the functional category $c$
$f(d, n)$	Number of families with exactly $d$ members in a genome of size $n$
$f_c(d, n)$	Number of families belonging to the functional category $c$ with exactly $d$ members in a genome of size $n$
$\beta$	Exponent of the family-population histogram
$\beta_c$	Exponent of the family-population histogram restricted to category $c$
$\chi_c$	Probability to introduce a new family of the category $c$ (empirically quantified by the slope of $f_c$ vs. $f$ )
$\zeta_c$	Exponent of the scaling of the size of functional category $c$ vs. genome size $n$



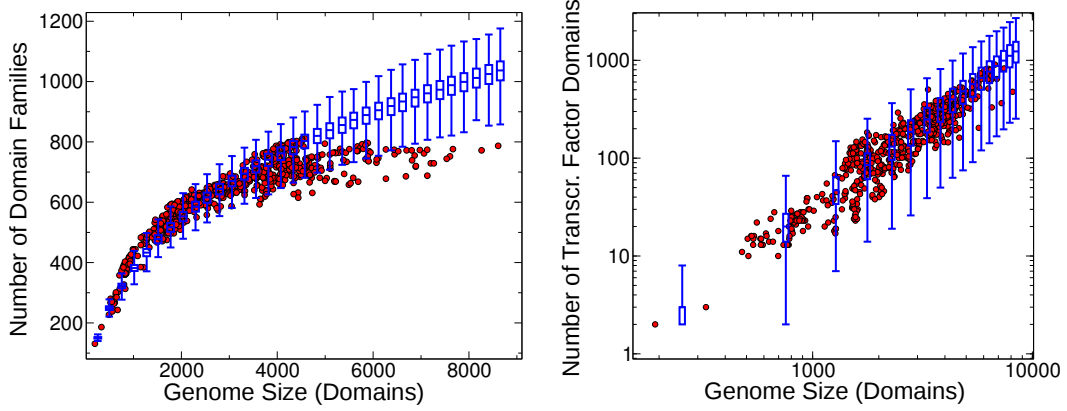


**Figure 3.** Comparison between 1000 realizations of the correlated duplication model Ib at  $\alpha = 0.3$  and  $\theta = 140$  (blue boxplot) with empirical data (red). The left panel is a plot of the number of distinct domain families versus genome size. The fact that the number of families does not saturate is a property of the standard duplication-innovation model (see [6] for a complete discussion). The right panel plots the number of TF domains versus the total number of domains, showing that the scaling of the transcription functional category is well reproduced (exponent  $\simeq 1.6$ .) See Supplementary Figure S4 for model Ia.

### Prediction of the exponents of the family-population histogram restricted to single functional categories.

While the agreement between model and data shows that the scaling of functional and evolutionary categories can be understood jointly, it does not provide by itself any substantially new information about how the two partitionings interact. Further insight can be obtained considering the distributions of the number of domains per family for different evolutionary families belonging to the same functional category. In general, the population of domain families of a genome follows a near power law distribution whose slope depends on genome size (Figure 4). The mean number  $f(d, n)$  of domain families having  $d$  members at large genome size  $n$  is well described by the slope  $1/d^{1+\beta}$  (see Figure 4), and thus the cumulative histogram by  $Q(d, n) \sim 1/d^\beta$ , where the fitted exponent  $\beta$  typically lies between 0 and 1. The standard CRP predicts this behavior [6, 14]. The model described here allows to consider the same histograms restricted to specific functional categories (Figure 4 and Figures 6).

A mean-field calculation (see Supplementary Text) based on the model variant with correlated duplication predicts that the different trend of domain population histograms for transcription-factor families scales as  $f(d, n)_{TF} \sim 1/d^{1+\frac{\beta}{2}}$  (see Figure 5). Thus, the ratio between the exponent of the cumulative histogram of all families and the exponent of the cumulative histogram restricted to families belonging to the transcription factor category is predicted to be equal to the mean-field exponent for the scaling of the functional category. Specifically,  $Q(d, n)$  scales as  $1/d^\beta$  whereas  $Q_{TF}(d, n)$  scales as  $d^{-\beta/2}$  and thus the ratio of exponents is  $\beta/(\beta/2) = 2$ , and this matches the asymptotic scaling of the number of transcription factors. More in general, the model indicates that each time the per-family duplication probability for a functional category takes the form  $p_O^c \simeq \zeta_c n_c$ , where  $n_c$  is the total population of the functional category  $c$ , the coefficient  $\zeta_c$  will appear in the equation for  $P(d)_c$ , the (cumulative) distribution of families belonging to category  $c$ . This causes the relationship  $\beta_c = \beta/\zeta_c$  and appears to be robust with respect to the choice of a specific model (see Supplementary Text). In other words, a precise quantitative relationship must exist between the scaling exponent of a category and the slope of the family population histogram restricted

to the same category. Functional categories that grow faster-than-linearly with genome size will have flatter-than-average domain family size distributions. Conversely categories growing slower-than-linearly will follow a steeper-than-average slope.

Accordingly, a strongly visible trend should be expected in empirical data from families belonging to the transcription factor category, which scales with exponent 2. Indeed, the empirical population histograms for the transcription factor functional category for all the genomes in the data set have a slope that is spectacularly different from the global one (Figure 5 and Supplementary Figure S13). Quantitatively, this observation is in excellent agreement with predictions (Table 2). Direct simulations of the correlated model reproduce well both the behavior of the histograms at given size and the dependency on genome size (see Figure 4).

More generally, one can test the prediction  $\zeta_c = \beta/\beta_c$  with an empirical evaluation of many functional categories (Figure 6). The agreement of empirical data with the predicted behavior is reasonably good, keeping in mind that many functional categories are composed by few or poorly populated families, and in these cases the data might not follow a scaling law that is as clearly defined as the metabolism or the transcription factor categories.

## 4 DISCUSSION

### Population of evolutionary families of a given functional category

We have presented the first combined quantitative description of the partitioning of genomes in both evolutionary families and functional categories. The results show that a theoretical framework that correctly reproduces both the scaling laws for functional categories of genes/domains and the scaling laws for gene/domain families (numbers and histograms) is possible. Biologically, this finding can help us understand the large-scale architecture of a genome in terms of its functional content.

Analyzing the data in order to formulate the model, we found that the number of evolutionary domain families forming a functional category is linear in the total number of domain families (Figure 2). Thus, the genomic subdivision of evolutionary classes in functional categories appears to be arguably the simplest possible, if one disregards the class population. This ingredient was taken as an assumption for all the models considered here, which the data fully justify.

The model leads to the nontrivial prediction that connects the growth exponent of a functional category to the slope of the population family histogram restricted to the same category. In other words, the populations functional categories and evolutionary families of genes are connected by a simple quantitative law. Specifically, the ratio between the exponent of the cumulative histogram of all families

**Table 2.** Prediction of the exponent of the family-population histograms restricted to singular functional category. Comparison between expected and observed ratio of the exponent of the cumulative histogram of all families and the exponent of the cumulative histogram of transcription-factor families ( Figure 6 ), for the five largest bacteria in the SUPERFAMILY database. The ratio can be compared with the mean-field prediction of 2, or directly with the empirical exponent of the transcription factor functional category (1.6).

Genome	$\beta/\beta_{TF}$	$\zeta_{TF}$
<i>Sorangium cellulosum</i>	$1.72 \pm 0.1$	1.6
<i>Burkholderia xenovorans</i>	$1.63 \pm 0.08$	1.6
<i>Burkholderia</i>	$1.54 \pm 0.13$	1.6
<i>Solibacter usitatus</i>	$1.46 \pm 0.05$	1.6
<i>Bradyrhizobium japonicum</i>	$1.59 \pm 0.11$	1.6

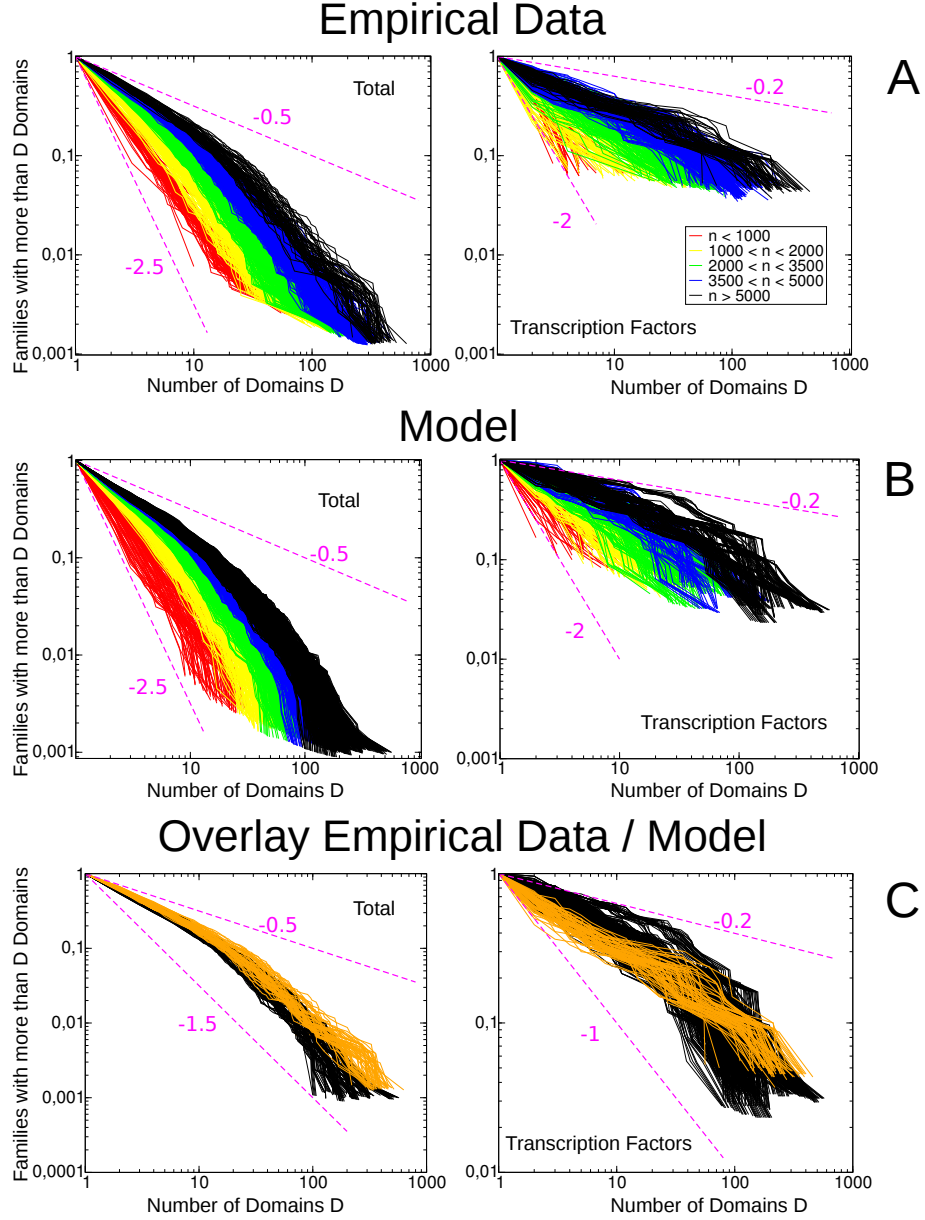


**Figure 4.** Empirical data and simulations for the normalized domain family population cumulative histograms. The histograms are defined as the fraction  $f(d, n)/f(n)$  of families with more than  $d$  domains. (A) Empirical data for the 753 bacteria in the SUPERFAMILY database (each color is a set of genomes with similar sizes). Left panel: domain family population cumulative normalized histograms. Right panel: normalized cumulative histograms restricted to domain families belonging to the transcription factor functional categories. Note that the histograms slopes are different. (B) Simulations for domains family population cumulative histograms of CRP with correlated duplications run at  $\alpha = 0.3$  and  $\theta = 140$ . The plots in the two panels are defined as in (A). (C) Comparison between simulations of the correlated duplication model variant run at  $\alpha = 0.3$  and  $\theta = 140$  (black lines) with empirical data (orange lines) for the largest genome sizes ( $5000 < n < 8500$ ). Left panel: global normalized cumulative histograms of domain family population. Right panel: normalized cumulative histograms restricted to transcription factor domain families.

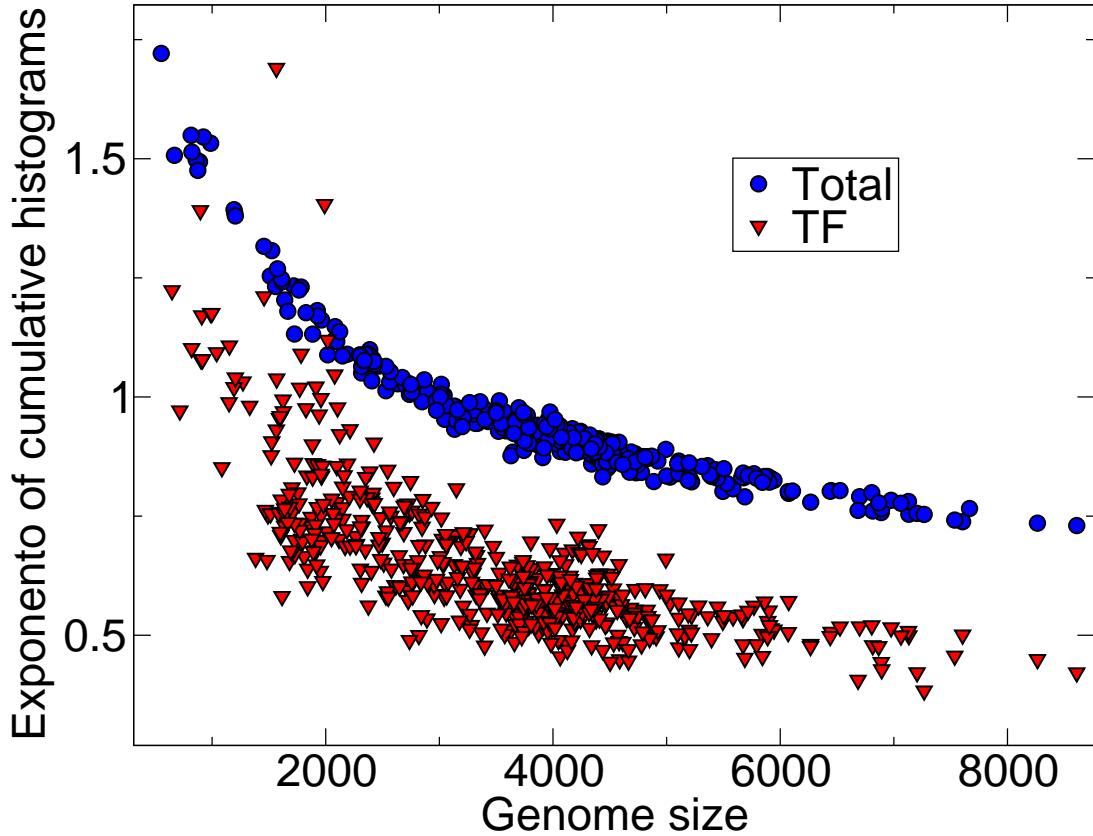


**Figure 5.** Exponent of evolutionary families and genome size. Fitted exponent of domain family population cumulative histograms vs. genome size, for the 753 bacteria in the SUPERFAMILY database for TF families (red circles) and all families (black squares), obtained by a fitting method giving a lower weight to the tail in order to keep into account the cutoffs (used in Ref. [14]).

and the exponent of the cumulative histogram restricted to families belonging to a functional category is predicted to be equal to the exponent for the scaling of the functional category.

To generate this prediction, we have analyzed in detail the case of transcription factors, where the exponent of the population histogram is halved due to the quadratic scaling using mean-field calculations and simulations, and verified that it holds in general by simulations of both model variants. Empirical data on transcription factors follow this behavior remarkably well, showing population cumulative histograms of transcription factor superfamilies decaying with halved exponents compared to the global populations. The fatter tails of the TF histograms might also be related to the fact that only a few highly populated DNA-binding domain superfamilies dominate the population of TF DNA-binding domains and determine the scaling laws (Supplementary Text and Supplementary Figures S10 and S11). More in general, we have also compared the behavior of domain family population histograms for all the empirical functional categories with the prediction, obtaining results that are in good agreement (Figure 6), in particular for the highly populated categories, where the fitting procedure gives the highest confidence. The only highly-populated category that significantly violates this general trend is small molecule binding, a category composed of very few highly-populated domain families. This category is known to follow peculiar evolutionary laws, with high mobility of domains across the metabolic network, resulting in members of

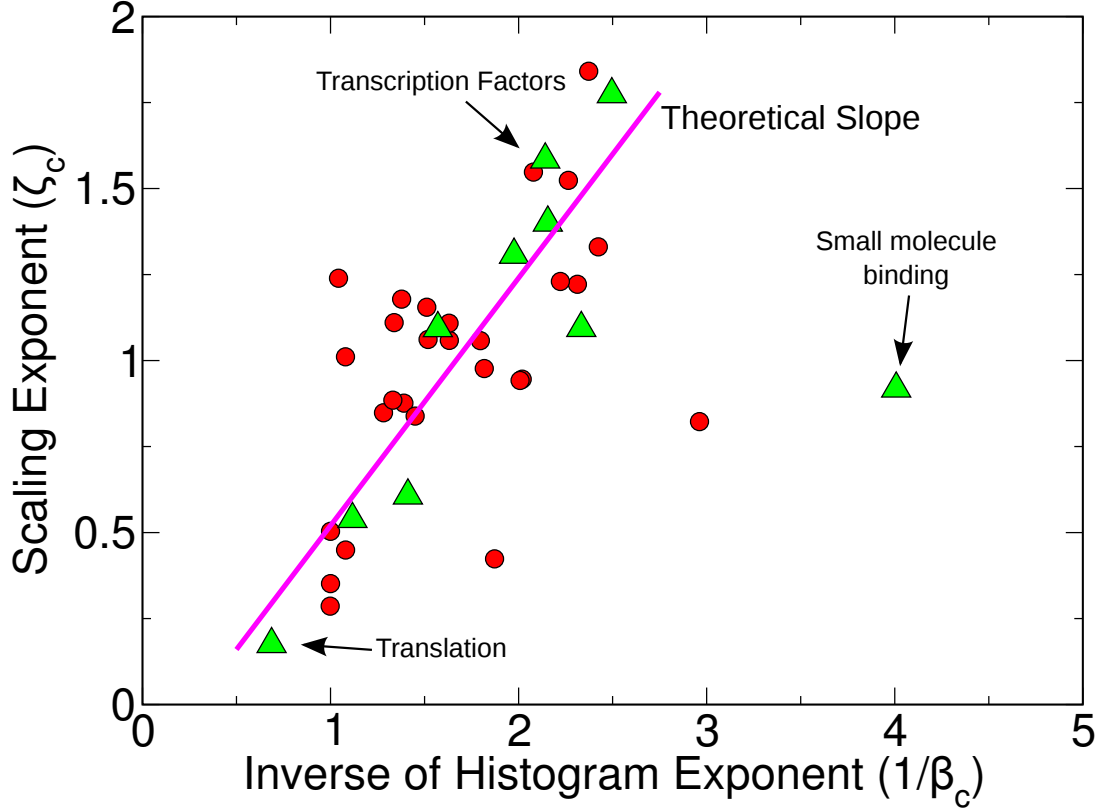


**Figure 6.** Linear relation between  $\zeta_c$  and  $1/\beta_c$ . Our theory predicts  $\zeta_c \sim \beta/\beta_c$  (solid line). The empirical value of  $\beta = .74$  is calculated from the family population histograms of the five most populated genomes. Symbols (circles and triangles) are empirical data for 38 functional categories (see also Supplementary Table S2). Triangles represent the ten most populated categories, where the estimated exponents are most accurate. The outlier is the “small molecule binding” category known to follow peculiar evolutionary mechanisms [20].

the same family being scattered across different pathways and producing lineage-specific domain families, with frequent re-invention of the same function by different families [20,21]. Thus, the exception makes biological sense, and can be understood in terms of members of evolutionary classes “jumping” to different functional categories with high rate during evolution.

### Correlated and absolute recipes

The central ingredient of our main model (model I) is the coupling between addition/removal of genes in different functional categories. From a biological standpoint, it is reasonable that gene repertoires of functional categories related to each other via shared tasks, pathways or processes should follow coordinated rules [8]. In order to further justify this assumption, we probed directly the empirical domain data for correlation between number of domains in different functional categories. To this end, for each genome  $g$  we calculated the deviation  $\delta n_c(g)$  between the functional category size ( $n_c(g)$ ) and its average size in genomes of comparable size (see Methods). We then calculated the matrix of correlations between values of  $\delta n_c$  for different functional categories  $c$ . The results are reported in Figure 7 and

Supplementary Tables S3 and S4. We also tested that this procedure for evaluating the correlation was not dependent on genome size (Supplementary Figure S9.) The metabolism categories appear to be highly (anti-)correlated with each other, probably because of the role they play in different pathways of a common metabolic network [15]. The observed correlations between metabolic families might also be relevant for reproducing the correct tail of the family population histogram restricted to the metabolism category (Supplementary Figure S3).

An alternative approach is a description where the growth of each category is governed by intrinsic “evolutionary potentials” [3]. We have also analyzed such a description in some detail (see Supplementary text and Supplementary Figure S3). Despite of minor differences, a model combining class-expansion/duplication/loss with uncorrelated moves for the functional categories, model II, can also perform well in reproducing the joint scaling law and in predicting a relationship between the scaling exponents and the functional categories. In particular, this means that the latter result should not by itself be considered a piece of evidence in favor of a correlated recipe. Figure 8 illustrates the basic differences between the two descriptions. The evolutionary potentials approach generically requires a lower number of parameters, but suffers from the tedious technical problem that the values of the growth coefficients cannot be controlled directly, because of the scaling of the normalization constant with genome size (see Supplementary Text and Supplementary Figure S7). The correlated model is technically more under control, since its behavior does not rely on any unknown normalization constant. For this reason, it also performs better with functional categories that grow faster than linear with genome size, such as transcription factors. On the other hand, such a model can be formulated with very few parameters only when a synthetic description for the correlations, such as the toolbox model, is provided.

Here, we have considered mainly a model with three categories (transcription factors, metabolic, and others) and one nonzero correlation between metabolic domains and transcription factors. In general, specific biological details of how categories are correlated with each other determine the scaling exponents relating their genome fractions to each other and genome size. Note that the task of formulating a correlated model for many categories requires a knowledge of how the different functional categories are “slaved” to each other. This structure is largely unknown quantitatively, and can in principle define an arbitrarily complex network of interactions, since many categories may correlate with many others in potentially complicated ways. Should the importance of correlated recipes be confirmed by further analysis, it seems likely that the full formulation of such a description would still require to solve this problem. In order to show explicitly that the model can in principle be successfully extended to many categories (and still give scaling laws) we have analyzed the case of a simple hierarchical structure where many categories are slaved to a main one (see Supplementary Figure S8).

Overall, since functional categories scaling laws effectively emerge from the correlated approach, a good reconciliation of the two approaches could be to interpret the evolutionary potential model as an emergent description (which can be very useful in concrete empirical applications). In other words, evolutionary potentials would describe emergent effective growth of functional categories of a genome, averaging over more “microscopic” evolutionary processes where addition of genes belonging to specific functional categories needs to comply to constraints combining different functions to perform specific cell tasks. These kind of interactions between functions are better described by correlated growth of functional categories. In this view, genome growth would be governed by a relative recipe, where the proportions are more important than the exact amounts, rather than an absolute recipe, where only the detailed amounts of each ingredient play a role.

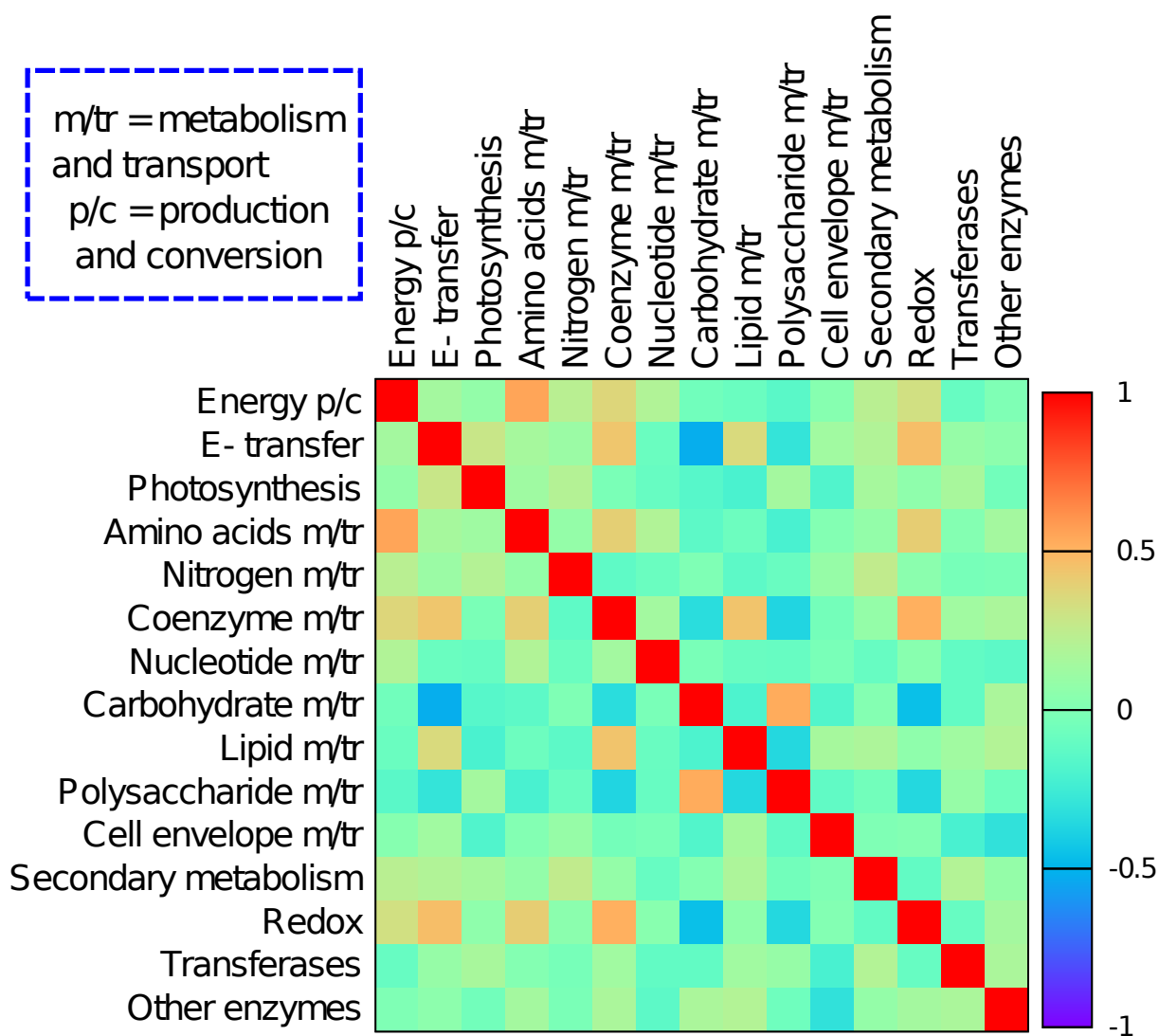


**Figure 7.** Correlation between the populations of 24 different metabolic functional categories from the SUPERFAMILY database for 753 bacteria. The correlation matrix is calculated from fluctuations of categories from the average trend (see Methods). Both correlation and anticorrelation are present between categories. Different metabolism categories are highly (anti-)correlated.

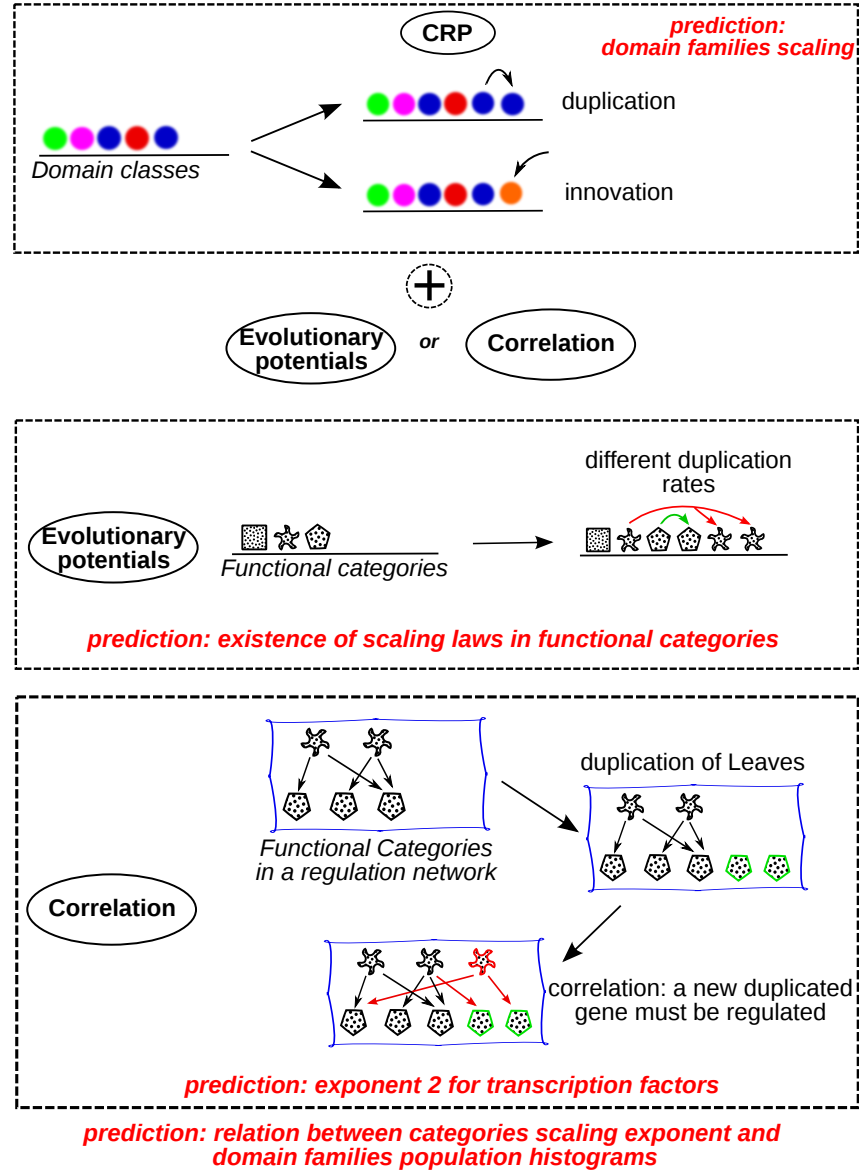


**Figure 8.** Models with correlated versus absolute moves. Top: the Chinese restaurant process (CRP) acts on the homology families (colors) with a duplication and an innovation move. It is extended here to include functional categories (shapes) Middle: model with evolutionary potentials. Functional categories are assigned differential duplication rates as in ref [3]. Bottom: Model with correlated moves. Members of the functional categories are added proportionally between correlated pairs of functions (e.g. transcription factors and metabolic targets) as in Ref. [15].



## References

1. Huynen, M. A. and van Nimwegen, E. (1998) The frequency distribution of gene family sizes in complete genomes.. *Mol Biol Evol*, **15**(5), 583–9.
2. van Nimwegen, E. (2003) Scaling laws in the functional content of genomes. *Trends in Genetics*, **19**(9), 479–484.
3. Molina, N. and van Nimwegen, E. (2008) The evolution of domain-content in bacterial genomes. *Biology Direct*, (3), 51+.
4. Koonin, E. V., Wolf, Y. I., and Karev, G. P. (2002) The structure of the protein universe and genome evolution.. *Nature*, **420**(6912), 218–23.
5. Dokholyan, N. V., Shakhnovich, B., and Shakhnovich, E. I. (2002) Expanding protein universe and its origin from the biological Big Bang.. *Proc Natl Acad Sci U S A*, **99**(22), 14132–6.
6. Cosentino Lagomarsino, M., Sellerio, A., Heijning, P., and Bassetti, B. (2009) Universal features in the genome-level evolution of protein domains. *Genome Biology*, **10**(1), R12+.
7. Perez-Rueda, E., Janga, S., and Martinez-Antonio, A. (2009) Scaling relationship in the gene content of transcriptional machinery in bacteria.. *Molecular Biosystems*, DOI: 10.1039/b907384a.
8. Koonin, E. V. and Wolf, Y. I. (2008) Genomics of bacteria and archaea: the emerging dynamic view of the prokaryotic world. *Nucleic Acids Research*, **36**(21), 6688–6719.
9. Treangen, T. J. and Rocha, E. P. C. (2011) Horizontal transfer, not duplication, drives the expansion of protein families in prokaryotes.. *PLoS Genet*, **7**(1), e1001284.
10. Karev, G. P., Wolf, Y. I., Rzhetsky, A. Y., Berezhovskaya, F. S., and Koonin, E. V. (2002) Birth and death of protein domains: a simple model of evolution explains power law behavior.. *BMC Evol Biol*, **2**(1), 18.
11. Qian, J., Luscombe, N. M., and Gerstein, M. (2001) Protein family and fold occurrence in genomes: power-law behaviour and evolutionary model.. *J Mol Biol*, **313**(4), 673–81.
12. Kamal, M., Luscombe, N., Qian, J., and Gerstein, M. (2006) Analytical Evolutionary Model for Protein Fold Occurrence in Genomes, Accounting for the Effects of Gene Duplication, Deletion, Acquisition and Selective Pressure. In Koonin, E., Wolf, Y., and Karev, G., (eds.), *Power Laws, Scale-Free Networks and Genome Biology*, pp. 165–193 Springer, New York.
13. Durrett, R. and Schweinsberg, J. (2005) Power laws for family sizes in a duplication model. *Ann. Probab.*, **33**(6), 2094–2126.
14. Angelini, A., Amato, A., Bianconi, G., Bassetti, B., and Cosentino Lagomarsino, M. (2010) Mean-field methods in evolutionary duplication-innovation-loss models for the genome-level repertoire of protein domains. *Phys. Rev. E*, **81**(2), 021919.
15. Maslov, S., Krishna, S., Pang, T., and Sneppen, K. (2009) Toolbox model of evolution of prokaryotic metabolic networks and their regulation. *Proceedings of the National Academy of Sciences*, **106**(19), 9743–9748.
16. Isambert, H. and Stein, R. (2009) On the need for widespread horizontal gene transfers under genome size constraint.. *Biology Direct*, **4**(1), 28+.

17. Bornberg-Bauer, E., Beaussart, F., Kummerfeld, S. K., Teichmann, S. A., and Weiner, J. (2005) The evolution of domain arrangements in proteins and interaction networks.. *Cell Mol Life Sci*, **62**(4), 435–45.
18. Wilson, D., Madera, M., Vogel, C., Chothia, C., and Gough, J. (2007) The SUPERFAMILY database in 2007: families and function. *Nucleic Acids Res*, pp. D308–D313 Updated 7/2009.
19. Pitman, J. (2006) Combinatorial Stochastic Process, Notes for St. Flour Summer SchoolSpringer-Verlag, Berlin.
20. Anantharaman, V., Koonin, E. V., and Aravind, L. (2001) Regulatory potential, phyletic distribution and evolution of ancient, intracellular small-molecule-binding domains.. *J Mol Biol*, **307**(5), 1271–1292.
21. Chothia, C., Gough, J., Vogel, C., and Teichmann, S. A. (2003) Evolution of the protein repertoire.. *Science*, **300**(5626), 1701–1703.
22. Charoensawan, V., Wilson, D., and Teichmann, S. A. (2010) Genomic repertoires of DNA-binding transcription factors across the tree of life. *Nucleic Acids Research*,.

## Supplementary Text and Figures for Grilli *et al.*

### S1 Description of the model and basic mean-field results

This section discusses in more detail the analytical derivation of the scaling for the main observables of model I and II using a mean-field approach.

Consider a joint partitioning of elementary units (domains or genes) in functional and evolutionary categories, as illustrated in Figure 1 of the main text. The elementary units (in our case domains), belong to a single evolutionary family  $i$ , and every family  $i$  belongs to one and only one functional category  $c$ .

The generic stochastic growth model considered here defines how new units are introduced into the system. The model is specified by a set of basic rates. The basic set of rates is constituted by the probabilities  $p_i$  that a newly added unit belongs to a certain class  $i$ . More in detail, we define a probability  $p_O^i$  (where  $O$  stands for “old”) that a new domain belongs to a family  $i$  which is already present in the system (i.e. having at least one member) and the probability  $p_N$  (where  $N$  stands for “new”) that the added unit belongs to a family which is not already present in the system.

The choice of  $p_O^i$  and  $p_N$  defines the model as a stochastic process for the basic observables (such as genome size  $n$ , family number  $f$  and its population  $n_i$ , etc.), but one extra detail is needed. When a new class is introduced, the model needs to specify the category it belongs to. As discussed in the main text, in the model considered here a newly added family always belongs to a category  $c$  with probability  $\chi_c$ . The probabilities  $p_O^i$ ,  $p_N$  and  $\chi_c$  can depend, in principle, on the number of units  $n$  and on their distribution in families, on the total number of families  $f$  and so on. Empirical data indicate (see Figure 2 in the main text) that  $\chi_c$  is a category-dependent constant, and thus does not depend on  $n$ .

The mean-field approximation is useful to extract the basic information from the model [6]. In each realization of the full stochastic process, the probabilities of the possible configurations at time  $t + 1$  are determined by the configuration at time  $t$ . The mean-field approximation assumes that the configuration at time  $t$  is the average configuration. For example, if one is interested in the number of domains belonging to family  $i$ , the average number of elements  $n_i(t + 1)$  at time  $t + 1$  will be equal to the average number of elements  $n_i(t)$  at time  $t$  summed with the average number of elements added in a time step, i.e.  $p_O^i$ . For asymptotically large  $t$  this implies the approximate equation  $\partial_t n_i = p_O^i$  for the averages (here the averaging procedure is implicit in the notation). Since typically, at each step one and only one element is added, the mean number of elements is  $n = t$ . If this is not the case, we can obtain  $\partial_n n_i$  simply from  $\partial_t n_i$  divided by  $\partial_t n$ . Considering  $n = t$  we obtain, for a generic model, the following mean-field equations

$$\begin{aligned}
 \partial_n n_i &= p_O^i \\
 \partial_n f &= p_N \\
 \partial_n f_c &= \chi_c p_N \\
 \partial_n n_c &= \partial_n \sum_{i \in c} n_i = \sum_{i \in c} \partial_n n_i + \partial_n f_c = \sum_{i \in c} p_O^i + \chi_c p_N .
 \end{aligned} \tag{S1}$$

#### S1.1 Models with correlations

We now deal with the scaling of the basic observables in the model taking into account the correlation between categories growth (model I of the main text).

The correlation appears in the growth of the domain families of different categories. Thus the probability  $p_O^i$  that a domain is added to a given family  $i$  can be written as

$$p_O^i = \frac{\sum_{j=1}^f a_{i,j} n_j - \alpha}{\sum_{i,j=1}^f a_{i,j} n_j + \theta} . \quad (\text{S2})$$

The coordinated growth of functional categories is encoded by the coefficients  $a_{i,j}$ , responsible for the correlated expansion of evolutionary families  $i$  and  $j$  (See Equation 1 of the main text). The standard Chinese Restaurant Process (CRP) is obtained by imposing  $a_{i,j} = \delta_{i,j}$  (where  $\delta_{i,j}$  is equal to 1 if  $i = j$  and 0 otherwise). We assume that these coefficients depend only on the functional categories  $c$  and  $c'$  to which the families  $i$  and  $j$  belong. The probability of introducing a new domain is given by

$$p_N = \frac{\alpha f + \theta}{\sum_{i,j=1}^f a_{i,j} n_j + \theta} . \quad (\text{S3})$$

### S1.1.1 Model Ia.

We consider a model inspired by ref. [15] (the toolbox model, in which the growth of the number of transcription factors is coupled to the number of added metabolic enzymes), extended to describe a joint partitioning in functional and evolutionary categories. In the original version of the model the average increment of the main observables at each time step is

$$\begin{cases} \Delta n_{met} = \frac{U}{n_{met}} \\ \Delta n_{TF} = 1 , \end{cases} \quad (\text{S4})$$

and thus  $\Delta n_{TF} / \Delta n_{met} = n_{met} / U$ , which gives a quadratic scaling for  $n_{TF}$  with  $n_{met}$ .

Model Ia is an extension of the toolbox model is formulated following equation S2, by using a proper definition of  $a_{i,j}$ , such as the same equation of the toolbox model is valid. We observe that, for our purpose, the time step of equation we can be defined arbitrarily, as genome growth is eventually parameterized by  $n$ . Rewriting the equations as

$$\begin{cases} \Delta n_{met} = n_{met} \\ \Delta n_{TF} = n_{met} \frac{n_{met}}{U} , \end{cases} \quad (\text{S5})$$

gives the summed probabilities  $p_O^i$  relative to the two categories

$$\begin{cases} p_O^{met} := \sum_{i \in met} p_O^i = \frac{n_{met} - \alpha f_{met}}{C(n)} \\ p_O^{TF} := \sum_{i \in TF} p_O^i = \frac{\frac{n_{met}}{U} n_{met} - \alpha f_{TF}}{C(n)} , \end{cases} \quad (\text{S6})$$

while

$$p_N = \frac{\alpha f + \theta}{C(n)} . \quad (\text{S7})$$

Accordingly, we extend the model to an arbitrary number of families by the choice  $a_{i,j} = \frac{n_{met}}{U} \frac{n_i}{n_{TF}}$  if  $i$  is a  $TF$  family and  $j$  a metabolic family and zero otherwise. This gives

$$\begin{cases} p_O^i = \frac{\sum_{j \in met} \frac{n_{met}}{U} \frac{n_i}{n_{TF}} n_j - \alpha}{\sum_{i,j=1}^f a_{i,j} n_j + \theta} & \text{if } i \in TF \\ p_O^i = \frac{n_i - \alpha}{\sum_{i,j=1}^f a_{i,j} n_j + \theta} & \text{if } i \in met . \end{cases} \quad (\text{S8})$$

This model gives the asymptotic quadratic scaling of  $n_{TF}$  with  $n_{met}$  by definition, using the exact same argument as the toolbox model. Other results have been obtained numerically (see Supplementary Figure S4).

### S1.1.2 Model Ib.

This second formulation of a model with correlated recipe (model Ib) imposes a different correlation rule. For example, consider the model involving only two functional categories, transcription factors controlling metabolic processes and metabolic enzymes.

In this variant the coefficients  $a_{i,j}$  have both a diagonal and a non diagonal part,  $a_{i,j} = \delta_{i,j} + b_{i,j}$ . If  $b = 0$  the model is the standard Chinese Restaurant Process. For this reason, model Ib is simpler to treat analytically, exploiting previous results. This work focuses mainly on the case  $b_{i,j} = n_i/n_{met}$  if  $i$  is a family from the functional category of transcription factors and  $j$  is a family from the metabolic functional category (and  $b_{i,j} = 0$  otherwise).

In this case, the summed probabilities  $p_O^i$  relative to the two categories are

$$\begin{cases} p_O^i = \frac{n_i + \sum_{j \in met} \frac{n_i}{n_{met}} - \alpha}{\sum_{i,j=1}^f a_{i,j} n_j + \theta} & \text{if } i \in TF \\ p_O^i = \frac{n_i - \alpha}{\sum_{i,j=1}^f a_{i,j} n_j + \theta} & \text{if } i \in met. \end{cases} \quad (S9)$$

Using the definitions given in Equation S1, one can see that,

$$C(n)\partial_n n_{TF} = n_{TF} + n_{TF} - \alpha f_{TF} + C(n)\partial_n f_{TF} = 2n_{TF} - \alpha f_{TF} + \alpha f_{TF} + \theta \chi_{TF} = 2n_{TF} + \theta \chi_{TF}, \quad (S10)$$

while

$$C(n)\partial_n n_{met} = n_{met} - \alpha f_{met} + C(n)\partial_n f_{met} = n_{met} + \theta \chi_{met}. \quad (S11)$$

Hence, for large  $n$ , since  $\partial_n f_c = \chi_c p_N \simeq \alpha f_c$ , the terms in the r.h.s. of Equations (S10) and (S11) cancel, giving the effective equation,

$$\frac{dn_{TF}}{dn_{met}} \simeq \frac{2n_{TF}}{n_{met}}, \quad (S12)$$

and thus the scaling  $n_{TF} \sim n_{met}^2$ .

## S1.2 Model II (model with evolutionary potentials)

This section presents in more detail the uncorrelated version of the model for the joint scaling (model II), assigning evolutionary potentials [3]  $\rho_c$  to the functional categories, related to the probability that a gene added in a functional category is fixed by natural selection. This model is an example of an “absolute recipe”, since each category grows with an intrinsic rate  $\rho_c$ , summing up the growth of the families belonging to the given category. The rate  $\rho_c$  acts on family growth through the class-expansion move. The probability of class expansion of a family belonging to the category  $c$  is equal to

$$p_O^i = \frac{\rho_{c(i)} n_i - \alpha}{\sum_{j=1}^f \rho_{c(j)} n_j + \theta}, \quad (S13)$$

where  $\rho_{c(i)} = \rho_c$  if the evolutionary family  $i$  belongs to the functional category  $c$ . This model assumes that the value of  $\rho_c(i)$  depends only on the category to which family  $i$  belongs. The probability that a domain belonging to category  $c$  is added by class expansion is then

$$p_O^c := \sum_{i \in c} p_O^i = \frac{\rho_c n_c - \alpha f_c}{\sum_{j=1}^f \rho_{c(j)} n_j + \theta}. \quad (S14)$$

Equally, the probability that the new domain is introduced by an innovation move (i.e. it belongs to a new family) is equal to

$$p_N = \frac{\alpha f + \theta}{\sum_{j=1}^f \rho_{c(j)} n_j + \theta}. \quad (S15)$$

Under the assumption (confirmed by empirical data, see main text) that the growth of old functional categories by adding new homology families through the innovation move is uniform (i.e. that  $f_c = A_c + \chi_c f$ ), the probability that a new family belonging to the category  $c$  is added by an innovation move is

$$p_N^c := \chi_c p_N = \chi_c \frac{\alpha f + \theta}{\sum_{j=1}^f \rho_{c(j)} n_j + \theta} = \frac{\alpha f_c + \theta \chi_c}{\sum_{j=1}^f \rho_{c(j)} n_j + \theta}. \quad (\text{S16})$$

## Evolutionary potentials can reproduce the combined scaling laws at finite sizes.

We tested this model by a combination of mean-field analytical arguments and direct simulation.

The mean-field equations are obtained from Equation S1 by using Equations S13 and S15. The equation for the growth of the mean number of members  $n_c$  of a functional category can be obtained simply by summing on the homology families that belong to a given category,

$$\partial_n n_c = \frac{\rho_c n_c + \theta \chi_c}{C(n)}, \quad (\text{S17})$$

where  $C(n) \simeq \sum_i \rho_i n_i$ . If  $C(n) \sim n$ , equation (S17) corresponds to the evolution equation written by Molina and Nimwegen. Simulations of this model (see Supplementary Figure S7) confirm that this is the case. Thus, the mean-field argument predicts that this model can reproduce both scaling laws.

Also note that a rescaling of  $C(n)$  is equivalent to a rescaling of  $\alpha$ . Indeed, for large  $n$ ,  $p_N \simeq \alpha f / C(n)$  (and  $p_O = 1 - p_N$ ), so imposing  $C(n) \simeq qn$  is equivalent to dividing  $\alpha$  by the constant factor  $q$ . Thus, one can choose  $q = 1$  without loss of generality (by a rescaling of all the  $\rho_c$ ), and the solution for the population of a functional category will be  $n_c \sim n^{\rho_c/q}$  as in the Molina/Nimwegen model, and thus  $\zeta_c = \rho_c/q$ .

On the other hand, an important point regarding this model is that, asymptotically for any choice over the  $\rho_c$  set, the maximum large- $n$  exponent observed will be 1. Indeed, we can use the approximation  $C(n) = \sum_i \rho_i N_i \sim \rho_{\max} n^{\rho_c/q}$ , but  $C = qn$ , so that  $q = \rho_{c_{\max}}$ . This means that an exponent close to 2, such as that observed for transcription factors can only be obtained in a transient regime of the model. Furthermore, the change of the evolutionary potential of one functional category has repercussions on the other categories, as it implies a change in the normalization constant  $C$ . These facts make a direct identification of the value of the evolutionary potential with an intrinsic property of a single functional category difficult. They also make the direct identification of evolutionary potentials less straightforward (as it requires an arbitrary rescaling).

However, the above remarks have little practical importance, and the large- $n$  behaviour of the model does not really affect its performance at the relevant values of  $n$ . Numerical simulations show that at the empirical genome sizes, the scaling behaviour of the model can reproduce rather well the empirical one. For simplicity we have restricted to three main categories (transcription factors, metabolic genes and “others”) and we verified that in practice it is not hard to find a parameter set in good agreement with the empirical data on protein domains (Supplementary Figure S3). The general number of parameters to adjust increases with the number of functional categories that one needs to consider.

## S2 Exponents of family size distribution histograms

This section discusses the family size distribution histograms, as obtained from the mean-field approach. To fix the ideas, we will focus on model Ib, where the mean-field equations can exploit the known results from the CRP. It is possible to write a mean-field “flux equation” for the histograms [14], which implements the fact that each duplication adds a family with one extra member to the histogram count and subtracts a family with its previous population,

$$\partial_n f(d, n) = p_O(d-1, n) f(d-1, n) - p_O(d, n) f(d, n) + p_N \delta_{d,1} \quad (\text{S18})$$

where  $p_O(d, n) = \frac{d-\alpha}{n+\theta}$  is the probability that a family with  $d$  domains add a new duplicated member. The term  $p_N = \frac{\alpha f + \theta}{n + \theta}$  contains the innovation probability contributing to the growth of the number of families with one member. Note that the flow between families can be written as

$$\sum_{i \in \left\{ \begin{smallmatrix} \text{families with} \\ j \text{ domains} \end{smallmatrix} \right\}} \partial_n n_i = (d - \alpha) \frac{f(d, n)}{n + \theta}.$$

This equation requires an assumption on  $f(d, n)$  in order to be solved. We assume the ansatz  $f(d, n) = P(d)f(n)$  which is justified by both simulation and empirical data [14]. Using the fact that  $\partial_n f(n) = p_N$ , combined with Equation S18 gives the following equation for the probability of a family to have  $d$  members

$$\alpha P(d) = (d - 1 - \alpha)P(d - 1) - (d - \alpha)P(d) \quad , \quad (\text{S19})$$

which can be solved in discrete or continuous  $d$  to get

$$P(d) \sim \left( \frac{1}{d} \right)^{1+\alpha} . \quad (\text{S20})$$

This predicts the asymptotic behaviour of data and simulations (see Figure 6) with  $\beta = \alpha$ , where  $\beta$  is the asymptotic exponent of the family size distribution.

Let us now turn to the same distribution, restricted to transcription factors. In model Ib, the flux from transcription factor families caused by family expansion is caused by two separate contribution, the CRP standard one, plus additions of transcription factors to an existing family caused by the addition of a metabolic enzyme

$$p_O^i(n) = \frac{1}{C(n)} \left[ (n_i - \alpha) + \frac{n_i}{n_{met}} n_{met} \right] , \text{ if } i \in TF \quad (\text{S21})$$

i.e.

$$p_O^i(n) = \frac{1}{C(n)} [2n_i - \alpha] , \text{ if } i \in TF. \quad (\text{S22})$$

Thus, for the transcription factor families, the probability that a domain is added to a family with  $d$  members will be

$$p_O^{TF}(d, n) = \frac{1}{C(n)} [2d - \alpha] . \quad (\text{S23})$$

The quantity  $p_O^{TF}(d, n)$  is the probability that a new transcription factor domain is added to a family with  $d$  members. The flux equation for TF families can be obtained by substituting equation S23 in equation S18, (for  $d > 1$ )

$$C(n) \partial_n f_{TF}(d, n) = [2(d - 1) - \alpha] f_{TF}(d - 1, n) - [2d - \alpha] f_{TF}(d, n) \quad (\text{S24})$$

This is solved using the usual ansatz  $f_{TF}(d, n) = P_{TF}(d)f_{TF}(n)$  (as explained above it is confirmed by both data and simulations). Using  $f_{TF}(n) = \chi_{TF} f(n)$ , leads to the equation

$$\alpha P_{TF}(d) = (2d - 2 - \alpha)P_{TF}(d) - (2d - \alpha)P_{TF}(d) \quad , \quad (\text{S25})$$

which gives:

$$P(d)_{TF} \sim \left( \frac{1}{d} \right)^{1+\frac{\alpha}{2}} , \quad (\text{S26})$$

that is  $\beta = \alpha/2 = \beta/2$ . In the above calculation we have supposed again that the number of transcription factors is small with respect to the total number of metabolic enzymes.

Furthermore, it can be argued that this fact is more general. Indeed, each time the per-family duplication probability for the TF functional category will have the form

$$p_O^i \simeq 2n_i ,$$

when family  $i$  belongs to TF category, the coefficient 2 will appear in the equation for  $P(d)_{TF}$  modifying the exponent. In particular, this will also be true for models Ia (generalizing the toolbox model) and II (generalizing evolutionary potentials).

In other words, each time a functional category scales with a given exponent, it can be argued on rather general grounds that the exponent of the population histograms of the homology families that form it will be affected. It is possible to generalize this argument, and find a precise relationship between the scaling exponent of a category and the family population histogram (restricted to the same category). In other words, if  $\zeta_c$  is the scaling exponent of the category  $c$  and  $\beta_c$  is the exponent of the cumulative distribution histogram for the families belonging to category  $c$ , that is (see Equation S26):

$$P(d)_c \sim \left(\frac{1}{d}\right)^{1+\beta_c} ,$$

we suggest that  $\beta_c = \beta/\zeta_c$ . We tested this prediction in empirical data plotting  $1/\beta_c$  versus  $\rho_c$  in Figure 6 (Pearson correlation coefficient 0.47).

## S3 Comparison of models by numerical simulation

### S3.1 Correlated and absolute recipes

This section compares the correlated duplication and the evolutionary potential model variants. We considered a three categories model (TF, Metabolic and “other”).

The evolutionary potential model needs to supply three parameters  $\rho_c$ , while the correlated model needs to supply the correlation law between categories ( $a_{ij}$ ). We impose a correlation only between transcription factor and metabolic families with the correlated model Ib prescription, i.e.

$$a_{ij} = n_i/n_{met}, \tag{S27}$$

where  $i$  is a TF family and  $j$  Metabolic,  $a_{ij} = 0$  (no correlation) otherwise.

Figure S3 summarizes the results of this comparison. The correlated duplication model performs better in reproducing the behavior of the transcription factor category (both scaling law and histograms). Both models are unsatisfactory in reproducing the family population histogram of the metabolism families. This is probably caused by the fact that neither model include a correlation between metabolic families (Figure 7).

Figure S7 illustrates the behaviour of the normalization function  $C(n)$ .  $C(n)$  is linear with  $n$  in the range of empirical genome sizes (although the slope is not exactly 1). It becomes nonlinear at larger sizes, and its linear behavior is restored only at very large values of  $n$ .

### S3.2 Model I can reproduce a set of different exponents

Extending a model (with absolute or correlated recipe) to a large number of categories is not a simple task. In the case of an absolute recipe model, adding a new category  $c'$  (and thus introducing a new evolutionary potential  $\rho_{c'}$ ) generally requires, in order preserve the scaling of all the categories, a tuning of all the evolutionary potentials (both the old ones and the new one). This is due to the fact that all the evolutionary potentials appear in the normalization constant  $C(n)$  in the growth equation of each category (Equation (S13)). In a model with a correlated recipe, the main problem is related to the fact



that the interaction laws between categories are not known, they can be complex and possibly include feedback.

In order to produce the proof of principle that a model with correlated recipes can work with more than three categories, we considered a trivial generalization of model Ib to multiple categories that are slaved to a main one, and considered the question of whether this model would be able to reproduce an arbitrary set of scaling exponents for the categories.

We consider a correlation matrix  $a_{i,j}$  of the form  $\delta_{i,j} + b_{i,j}$ , where  $b_{i,i} = 0$ . This model deals with  $\mathcal{C}+1$  categories, the *met* category (in analogy with model Ib defined in the main text, this is a category whose growth is not conditioned to the others), and an additional set of  $\mathcal{C}$  categories labeled from 1 to  $\mathcal{C}$ . The non diagonal correlation coefficients  $b_{i,j}$  are zero if family  $i$  belongs to the *met* category, and  $\gamma_{c(i)} n_i / n_{met}$  if family  $i$  belongs to category  $c$ , different from *met*, and  $j$  belongs to the *met* category. Substituting this choice in equation S9, gives

$$\frac{dn_c}{dn_{met}} = (1 + \gamma_c) \frac{n_c}{n_{met}} \quad (\text{S28})$$

and thus

$$n_c \sim n_{met}^{1+\gamma_c}. \quad (\text{S29})$$

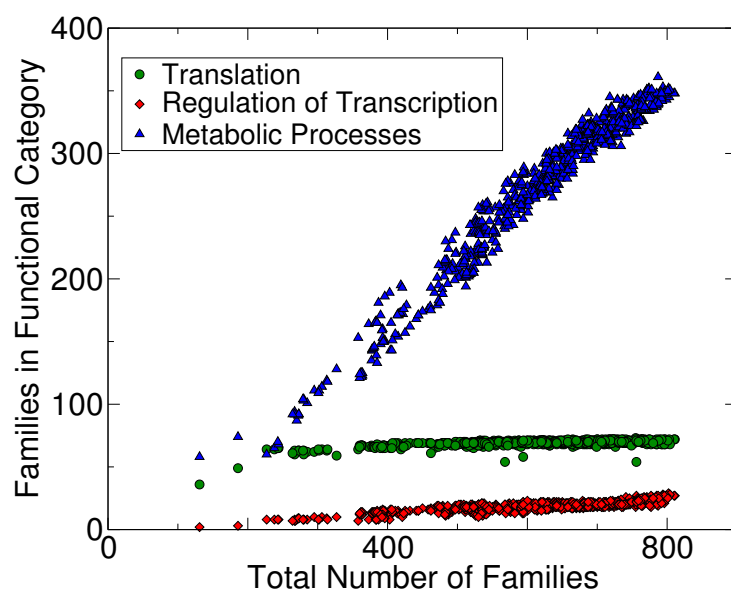
Supplementary Figure S8 shows simulations from a model with  $10 + 1$  categories. The model is able to reproduce an arbitrary set of exponents. We observe that this version has similar problems as the model with evolutionary potentials, as, in absence of a biological underlying model, it needs the tuning of a set of parameters to reproduce the scaling laws. The fitted exponent is typically different from  $1 + \gamma_c$ , specifically it seems to be closer to one. We interpret this as a finite size effect, due to the fact that the contribution of innovation to the scaling exponents is relevant.

## S4 Details of TF-domain superfamily scaling

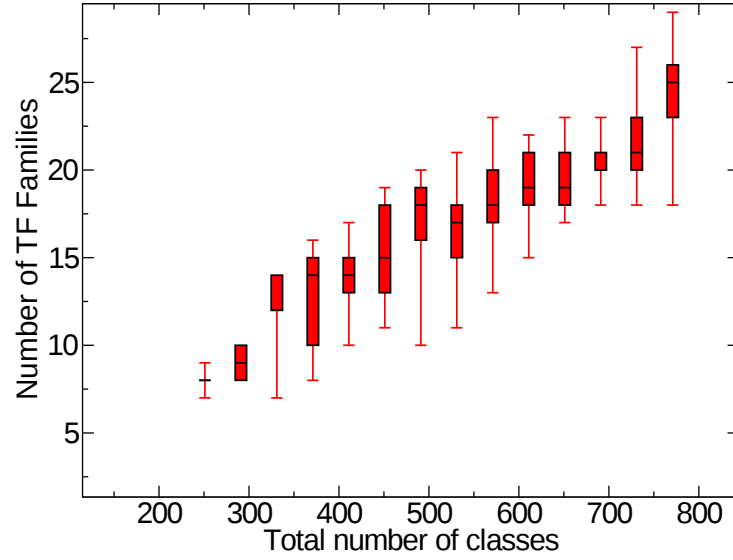
We observe that the quadratic (or very nearly so) scaling for transcription factors is clearly visible at in the two most populated families of transcription factor DNA-binding domains (Homeodomain-like and Winged-helix), which have a rather clean slope (see Supplementary Figure S10). In fact, three families present a clearly observable scaling alone (Homeodomain-like, Winged-helix and C-terminal), but just the first two follow a very nearly quadratic scaling.

Note however that removing the six most populated TF families, representing 80% of the total TF-domain population, the remaining ones considered together still present a scaling when added up, but with exponent  $\simeq 0.9$  (see Supplementary Figure S11). This indicates that the collective scaling of TF families cannot be entirely recunducted to properties of the most populated ones, but these are the families responsible for the *quadratic* scaling.

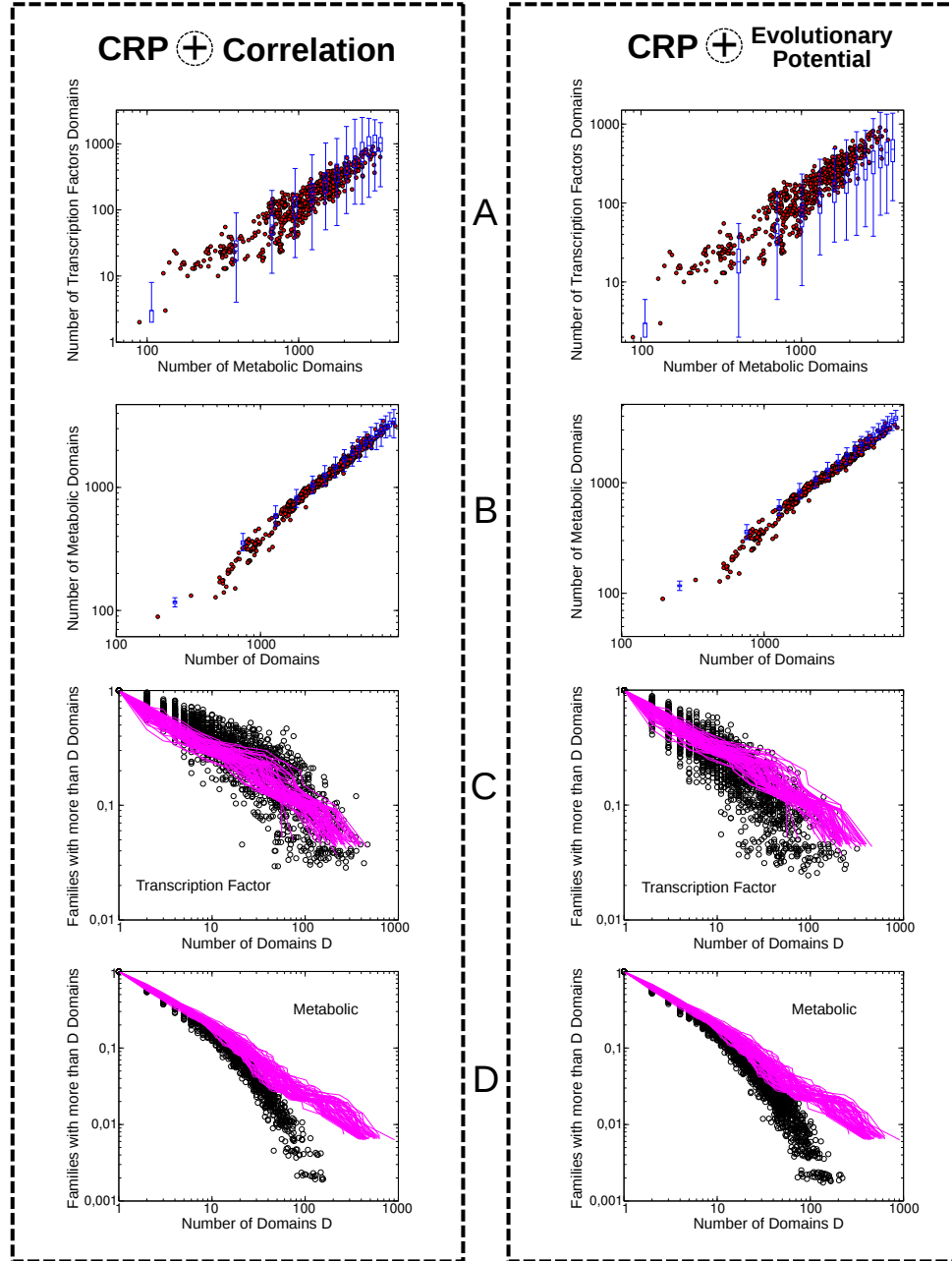
Thus, the “pure” quadratic scaling is observable in the largest transcription factor families. Collecting all the families, we measure a lower exponent in empirical data (close to 1.6). Supplementary Figure S11 explains this behavior, showing the total contribution of the smaller transcription factor families. These families collectively show a lower exponent (close to 1). Thus, we can interpret the lower collective exponent as an effect of family size (i.e., in the language of statistical mechanics, a “finite-size” effect) connected to the fact that for smaller family size, the innovation move is more relevant and thus the family expansion process is slower. The same effect is present in our simulations (see Supplementary Figure S12.)



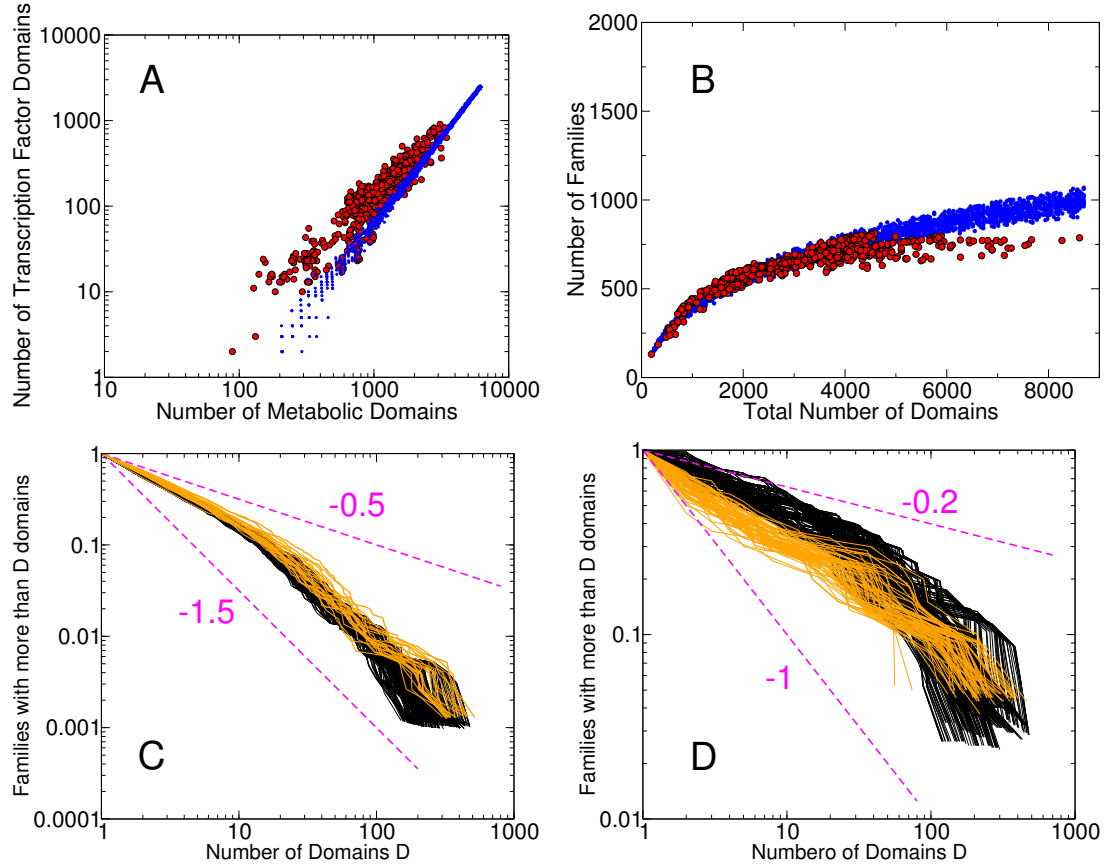
**Supplementary Figure S1. Scaling of the number of families in the three main functional categories.** Linear scaling behaviour of the number of families in three important functional categories versus total number of families from empirical data (for 753 bacteria in the SUPERFAMILY database). The slopes for the three linear laws are 0.01 (Translation), 0.03 (Regulation of Transcription) and 0.47 (Metabolic Processes).



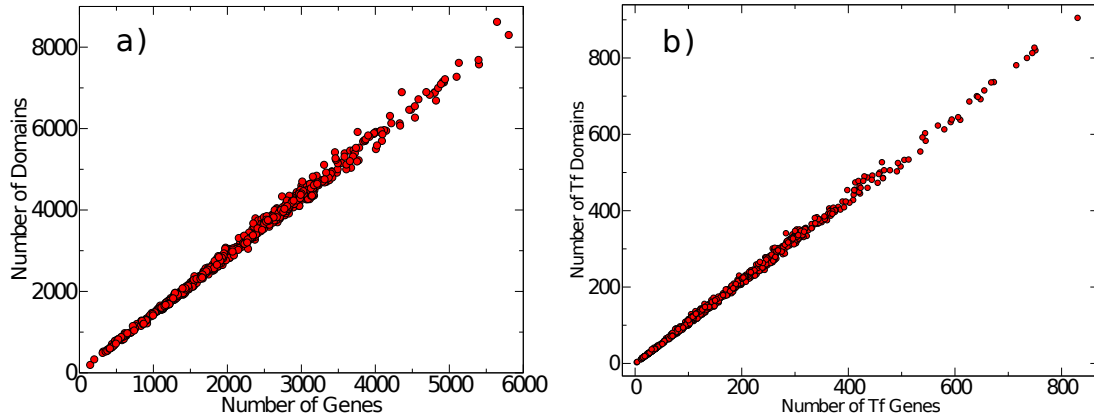
**Supplementary Figure S2. Transcription factor families.** Boxplot of the number of transcription factor domain families versus total number of domain families (data from 753 SUPERFAMILY bacteria). There appears to be a roughly linear scaling. This means that the number of TF domain families is compatible with a null hypothesis of independent addition model. Charoensawan *et al* [22] propose that the number of TF families follows a linear scaling with genome size. If this were to be the case, the innovation dynamics of transcription factor families should be distinct from other families. In fact, if  $f_{TF}(n) \sim n$ , since the total number of families is sublinear,  $f(n) \sim n^\alpha$  in the CRP (Figure 1), then one would have  $f_{TF} \sim f^{2-\alpha}$ , which is not confirmed by the SUPERFAMILY data analyzed here.



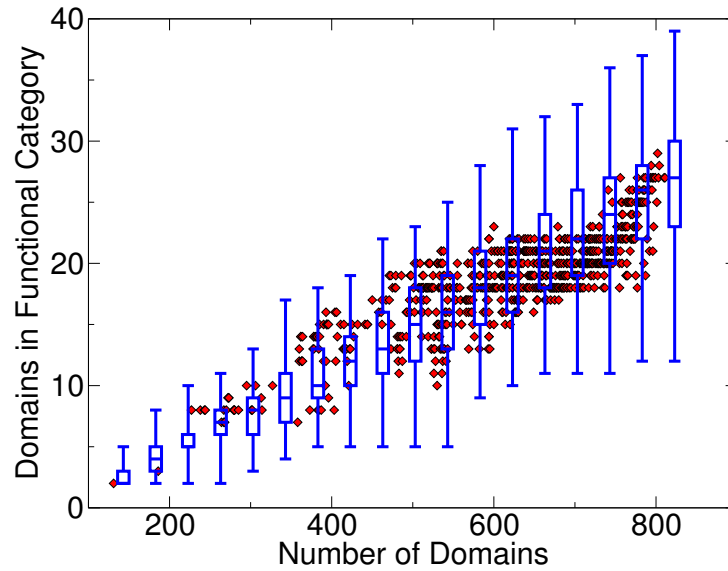
**Supplementary Figure S3. Comparison between models Ib and II.** Comparison between simulation of the correlated duplication model Ib (left panel) and evolutionary potentials (right panel) model variants with empirical data. Simulations are run at  $\alpha = 0.3$  and  $\theta = 140$ . (a) Number of TFs domains vs. number of metabolic domains (the blue boxplot corresponds to simulations, red circles to empirical data). (b) Number of metabolic domains vs. total number of domains (the blue boxplot corresponds to simulations, red circles to empirical data). (c) Family population histograms restricted to the transcription factor functional category (black circles are simulations, magenta lines empirical data). (d) Family population histograms restricted to the metabolism functional category (black circles are simulations, magenta lines empirical data).



**Supplementary Figure S4. Simulations of the correlated duplication model Ia for two categories (transcription factors and metabolic enzymes).** The plots are obtained from 1000 realizations with  $\alpha = 0.3$ ,  $\theta = 140$  and  $U = 7000$ . The observables are the same as in figure S3. (a) scaling of the number of transcription factors with the number of metabolic enzymes. (b) Number of families as a function of genome size  $n$ . (c) Family population (cumulative) histograms. (d) Family population histograms restricted to the families belonging to the transcription factor functional category.

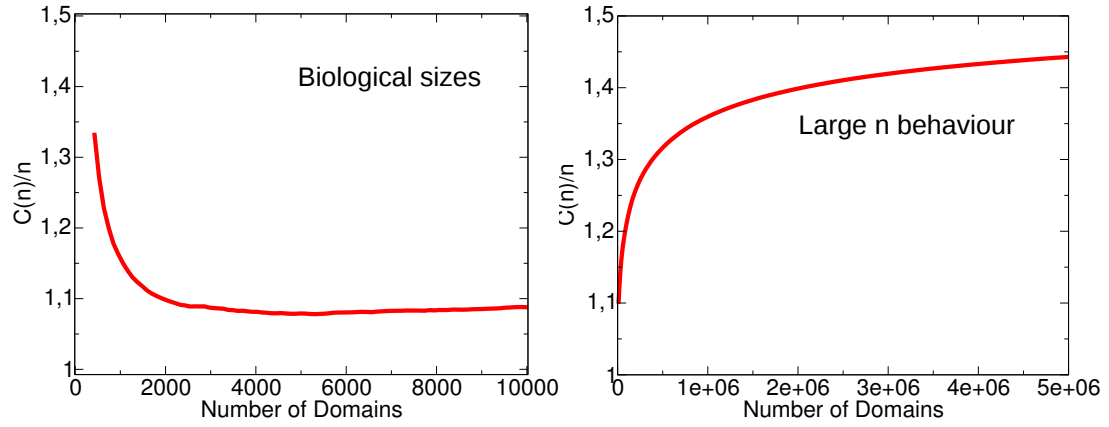


**Supplementary Figure S5. Linear relation between the number of domains and the number of genes.** (a) Number of Domains vs. number of protein-coding genes for the 753 bacteria in the SUPERFAMILY database. There are, on average, 1.45 domains per gene. (b) Linear scaling behaviour of the number of TF domains vs. number of TF genes. There are, on average, 1.09 TF domains in a TF gene.

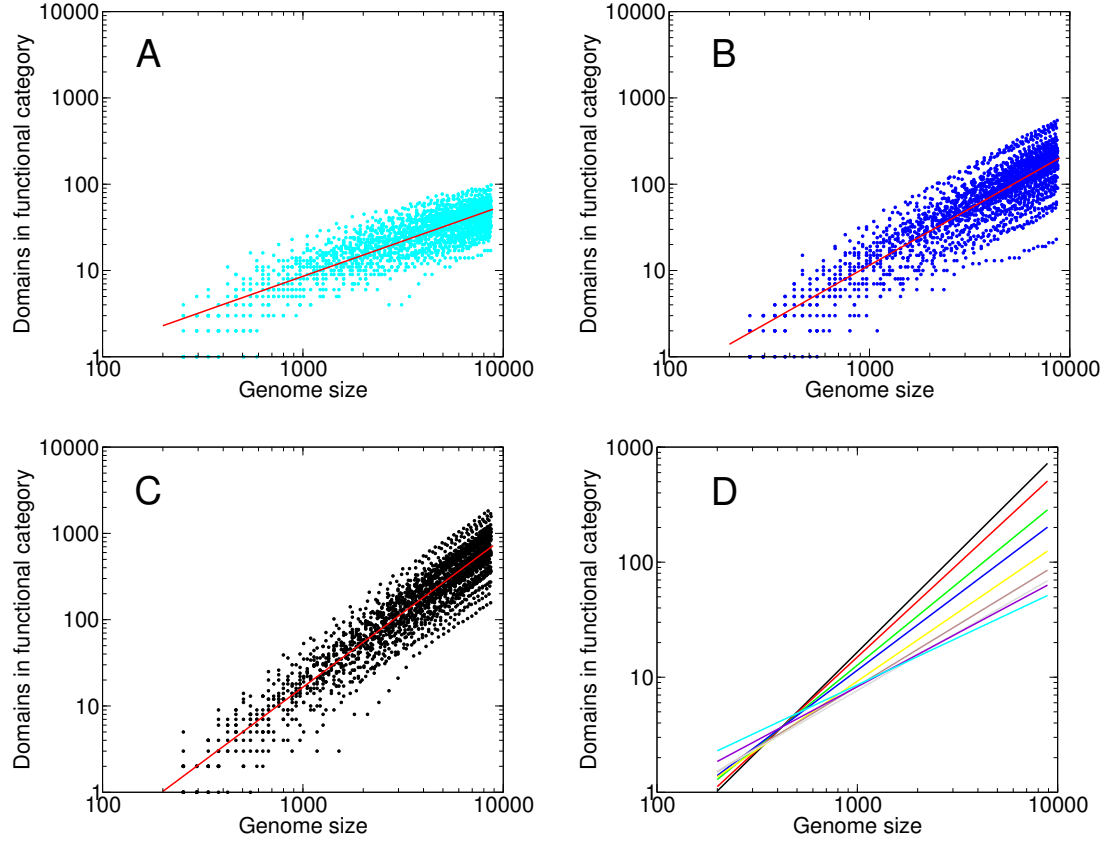


**Supplementary Figure S6. Simulation of the number of transcription factor families.**

Comparison between empirical data and simulations of the number of transcription factor domain families plotted against total number of families. The scaling is empirically linear, i.e. the number of TF domain families is reproduced by a null hypothesis of independent addition model. The choice of the parameter is 0.035.

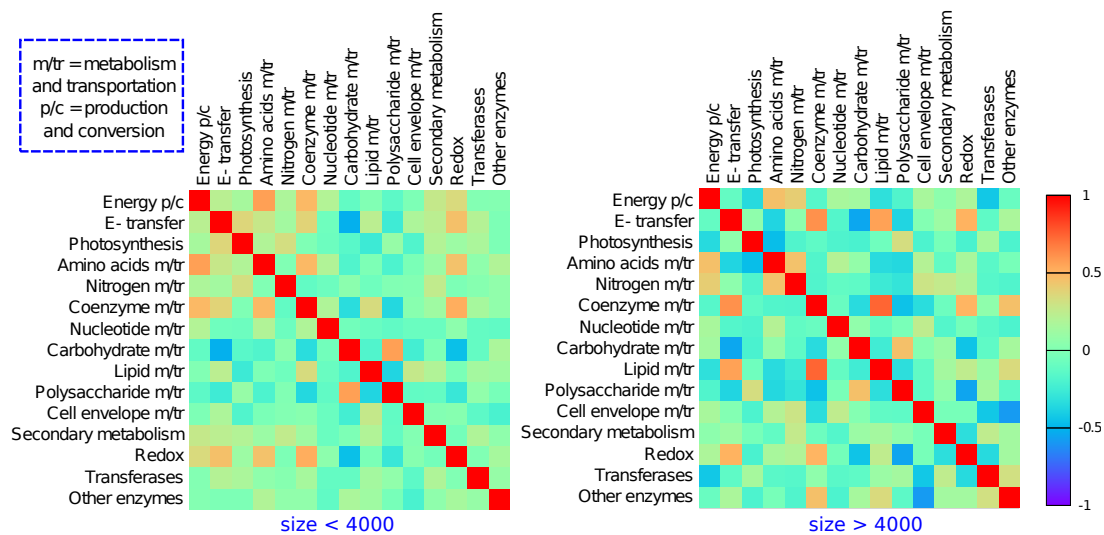


**Supplementary Figure S7. Normalization constant in the model with evolutionary potentials (model II).** Behavior of the ratio  $C(n)/n$ , where  $C(n)$  is the normalization factor for the evolutionary potential model. Data from simulations with three categories run at parameters  $\alpha = 0.3$  and  $\theta = 140$ .  $C(n)$  is linear with  $n$  in the range of empirical genome sizes, it then loses linearity, to become linear only asymptotically.

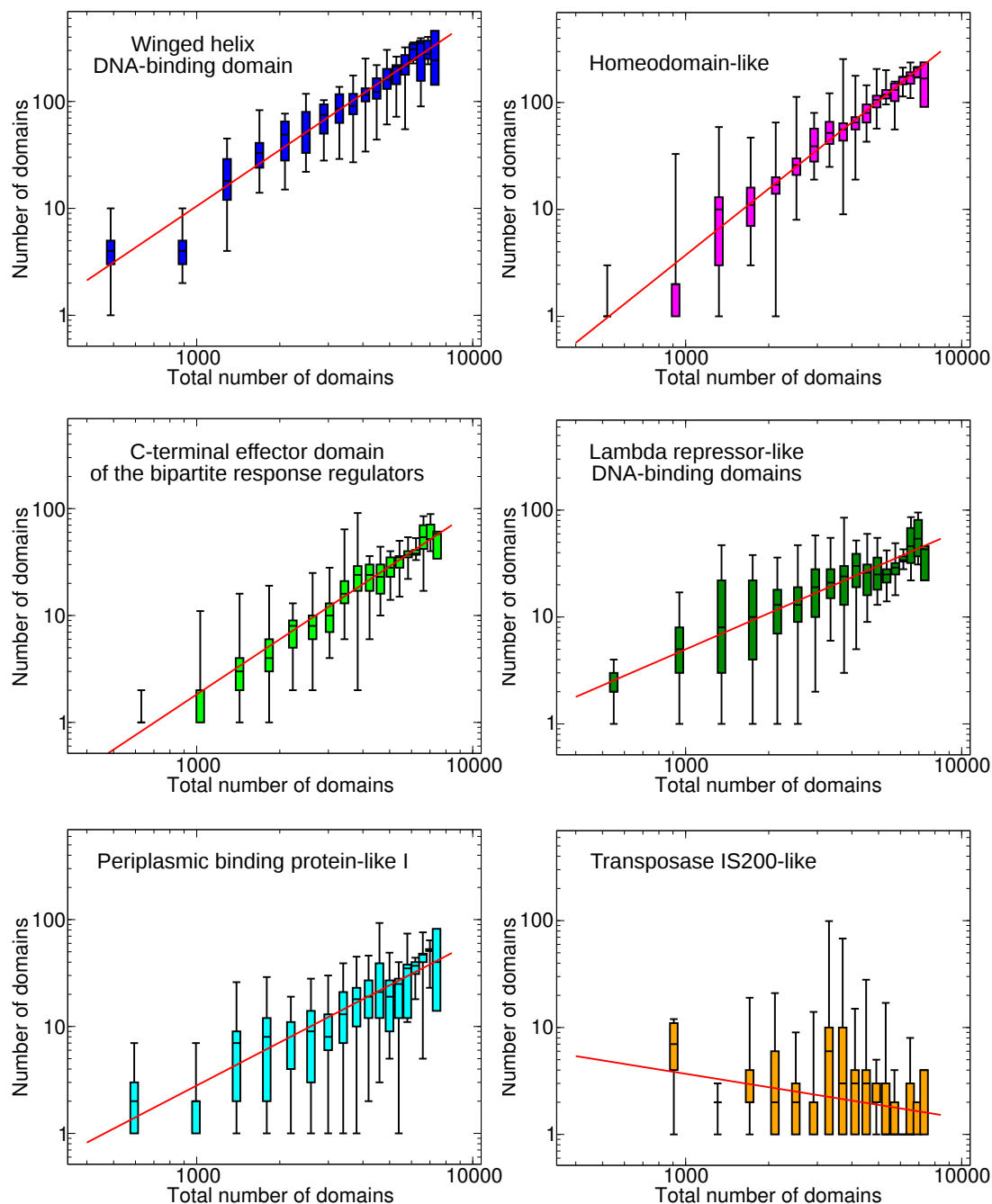


**Supplementary Figure S8. Simulation of model 1b with 10 + 1 categories.** 10 categories are slaved to one master category with different correlation laws, which determine the observed exponents). Panel A, B and C show the simulations of the population of three categories (respectively with  $\gamma_c$  equal to 1, 0 and  $-0.7$ ). The red lines are power-law fits of the simulated data. Panel D shows the power-law fits of the simulated data for all ten categories.

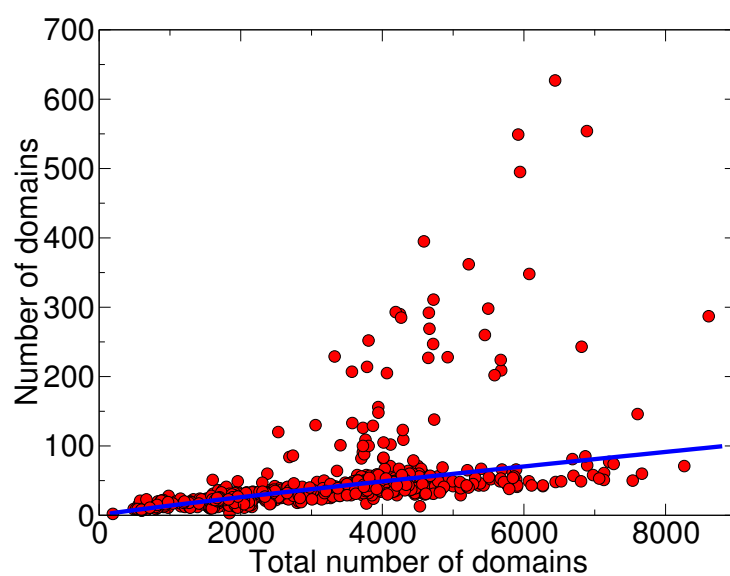




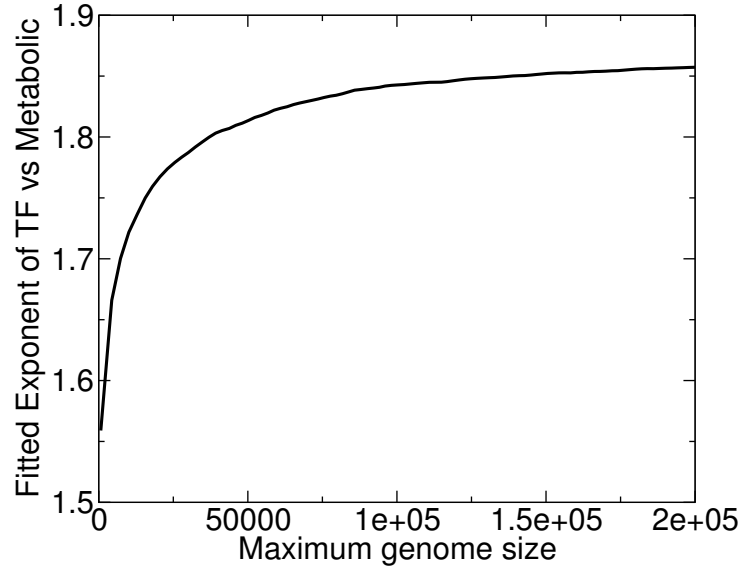
**Supplementary Figure S9. Correlation matrix for two sets of genomes with different sizes.** Left panel: Correlation matrix for genomes with size < 4000. Right panel: Correlation matrix for genome with size > 4000. The correlations do not depend on size.



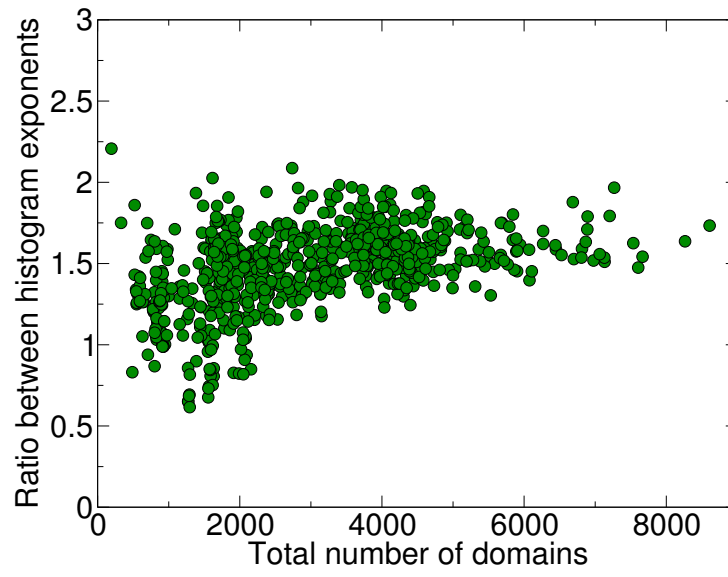
**Supplementary Figure S10. Most populated transcription factor superfamilies.** Boxplots for the population of the six most populated superfamilies of TF DNA-binding domains (y-axis in each panel) versus number of domains of each genome (x-axis in each panel). The presence of scaling laws appears likely for the three most populated families and arguable for the first five. Red lines represent best power law fit (1.8 for Winged Helix, 2.1 for Homeodomain-like and 1.7 for C-terminal effector)



**Supplementary Figure S11. Scaling of the least populated transcription factor superfamilies.** Collective scaling of the number of transcription factor domains after removing the six globally most populated families. While a few genomes show large fluctuations from the typical trend, a clear scaling is still observable for most genomes, with a fitted exponent equal to 0.9



**Supplementary Figure S12. MARCO Finite-size effects on the scaling exponent  $\zeta_{TF}$  for transcription factors in simulations of model Ib.** The plot shows the fitted exponent (y-axis) from the curve of the number of transcription factor domains versus the number of metabolic enzymes in 500 simulated realizations of model Ib with parameter  $\alpha = 0.3$  and  $\theta = 140$ . Each point on the x-axis corresponds to simulated data stopped at a given size  $n$ . The mean-field prediction ( $\zeta_{TF} = 2$ ) is reached only in the limit  $n \rightarrow \infty$ . This plot shows that the fitted exponent 1.6 (instead of 2) for the growth of transcription factors vs metabolic domains is due to a finite-size effect of a process that produces an exponent 2 in the large- $n$  limit. The same effect is present in models Ia and II.



**Supplementary Figure S13. Ratio between exponents of family population histograms.**

The plot reports the ratio  $\beta/\beta_{TF}$  between the exponent of the total family population histograms and the histograms restricted to the transcription factor families (see Figure 5 in the main text), as a function of genome size. The values of the ratio are distributed around 1.6 and the fluctuation range decreases with increasing genome size.

**Supplementary Table S1. Fitted values of  $\chi_c$  and offsets  $A_c$  from  $f_c$  vs  $f$  for the ten largest functional categories**

	$A_c$	$\chi_c$	Reduced chi square
Transcription Factors	$2.2 \pm 0.4$	$0.0267 \pm 0.0006$	4.5
Translation	$61.0 \pm 0.35$	$0.0133 \pm 0.0006$	3.9
Small molecule binding	$3.0 \pm 0.2$	$0.01 \pm 0.0002$	0.9
Nucleotide transport and metabolism	$5.6 \pm 0.3$	$0.02 \pm 0.0005$	3.1
DNA replication/repair	$9.5 \pm 0.6$	$0.0437 \pm 0.0009$	9.8
Inorganic ion transport and metabolism	$0.2 \pm 0.4$	$0.0272 \pm 0.0005$	3.5
Redox	$-7.6 \pm 0.5$	$0.0592 \pm 0.0008$	7.9
Transferases	$5.3 \pm 0.2$	$0.0213 \pm 0.0004$	1.6
Other enzymes	$-14.8 \pm 1.1$	$0.155 \pm 0.002$	35.7
Signal transduction	$-3.2 \pm 0.3$	$0.0282 \pm 0.0005$	3.3

The number of evolutionary families belonging to a functional category follows a linear law in empirical data. The table reports fits of  $f_c = A_c + \chi_c f$  from the plots in Figure 2 of the main text, where  $f_c$  represents the number of families in category  $c$  on all genomes and  $f$  is the total number of families on the genome. The third column is the reduced chi square.

**Supplementary Table S2. Data of fitted exponents from Figure 6 of the main text, for the ten largest functional categories**

	$\zeta_c$	$\beta_c$
Transcription Factors	$1.6 \pm 0.02$	$0.47 \pm 0.01$
Translation	$0.176 \pm 0.003$	$1.46 \pm 0.02$
Small molecule binding	$0.918 \pm 0.006$	$0.25 \pm 0.01$
Nucleotide transport and metabolism	$0.61 \pm 0.01$	$0.71 \pm 0.01$
DNA replication/repair	$0.54 \pm 0.01$	$0.9 \pm 0.01$
Inorganic ion transport and metabolism	$1.40 \pm 0.02$	$0.46 \pm 0.01$
Redox	$1.3 \pm 0.01$	$0.52 \pm 0.02$
Transferases	$1.09 \pm 0.01$	$0.43 \pm 0.01$
Other enzymes	$1.09 \pm 0.01$	$0.64 \pm 0.01$
Signal transduction	$1.77 \pm 0.03$	$0.4 \pm 0.01$

**Supplementary Table S3. Correlation coefficients between the populations of metabolic functional categories**

	En	e-	Ph	Aa	N	Co	Nu	Ca	Li	Ps	Ce	2M	Rx	Tr	Ot
En	1	0.14	0.07	0.55	0.23	0.36	0.19	-0.06	-0.08	-0.14	0.02	0.22	0.31	-0.10	-0.004
e-	0.14	1	0.29	0.15	0.11	0.43	-0.09	-0.52	0.35	-0.29	0.13	0.19	0.47	0.09	0.05
Ph	0.07	0.29	1	0.12	0.21	-0.02	-0.09	-0.16	-0.21	0.14	-0.18	0.15	0.06	0.16	-0.05
Aa	0.55	0.15	0.12	1	0.08	0.39	0.19	-0.14	-0.07	-0.22	0.01	0.07	0.40	0.02	0.14
N	0.23	0.11	0.21	0.08	1	-0.13	-0.08	-0.003	-0.14	-0.09	0.09	0.26	0.04	-0.03	-0.02
Co	0.36	0.43	-0.02	0.39	-0.13	1	0.14	-0.33	0.44	-0.37	-0.04	0.08	0.51	0.12	0.16
Nu	0.19	-0.09	-0.09	0.19	-0.08	0.14	1	-0.03	-0.09	-0.10	-0.02	-0.10	0.03	-0.11	-0.13
Ca	-0.06	-0.52	-0.16	-0.14	-0.003	-0.33	-0.03	1	-0.20	0.53	-0.18	0.02	-0.46	-0.11	0.16
Li	-0.08	0.35	-0.21	-0.07	-0.14	0.44	-0.09	-0.20	1	-0.35	0.15	0.18	0.06	0.13	0.20
Ps	-0.14	-0.29	0.14	-0.22	-0.09	-0.37	-0.10	0.53	-0.35	1	-0.12	-0.05	-0.36	0.09	-0.07
Ce	0.02	0.13	-0.18	0.01	0.09	-0.04	-0.02	-0.18	0.15	-0.12	1	-0.0002	0.01	-0.22	-0.31
2M	0.22	0.19	0.15	0.07	0.26	0.08	-0.10	0.02	0.18	-0.05	-0.0002	1	-0.11	0.20	0.08
Rx	0.31	0.47	0.06	0.40	0.04	0.51	0.03	-0.46	0.06	-0.36	0.01	-0.11	1	-0.10	0.14
Tr	-0.10	0.09	0.16	0.02	-0.03	0.12	-0.11	-0.11	0.13	0.09	-0.22	0.20	-0.10	1	0.17
Ot	-0.004	0.05	-0.05	0.14	-0.02	0.16	-0.13	0.16	0.20	-0.07	-0.31	0.08	0.14	0.17	1

Pearson's correlation coefficients between the populations of 24 different metabolic functional categories from the SUPERFAMILY database for 753 bacteria. Correlations are calculated from fluctuations of categories from the average trend (see Methods). Both correlation and anticorrelation are present between categories. Metabolism categories are highly (anti-)correlated. We used the following short forms for the metabolic functional categories: En = Energy p/c, e- = Electrons transfer, Ph = Photosynthesis, Aa = Amino acids m/tr, N = Nitrogen m/tr, Co = Coenzyme m/tr, Nu = Nucleotide m/tr, Ca = Carbohydrate m/tr, Li = Lipid m/tr, Ps = Polysaccharide m/tr, Ce = Cell envelope m/tr, 2M = Secondary metabolism, Rx = Redox, Tr = Transferases, Ot = Other enzymes. Where m/tr stands for "metabolism and transportation" and p/c means "production and conversion".

**Supplementary Table S4. P-Values of correlation coefficients between the populations of metabolic functional categories**

	En	e-	Ph	Aa	N	Co	Nu	Ca	Li	Ps	Ce	2M	Rx	Tr	Ot
En	0	$5 \cdot 10^{-5}$	<b>0.02</b>	$< 10^{-6}$	$< 10^{-6}$	$< 10^{-6}$	$< 10^{-6}$	0.05	<b>0.01</b>	$4 \cdot 10^{-5}$	0.26	$< 10^{-6}$	$< 10^{-6}$	$4 \cdot 10^{-3}$	0.46
e-	$5 \cdot 10^{-5}$	0	$< 10^{-6}$	$2 \cdot 10^{-5}$	$1 \cdot 10^{-3}$	$< 10^{-6}$	$8 \cdot 10^{-3}$	$< 10^{-6}$	$< 10^{-6}$	$< 10^{-6}$	$3 \cdot 10^{-4}$	$1 \cdot 10^{-6}$	$< 10^{-6}$	$7 \cdot 10^{-3}$	0.08
Ph	<b>0.02</b>	$< 10^{-6}$	0	$1 \cdot 10^{-3}$	$< 10^{-6}$	0.29	$2 \cdot 10^{-3}$	$< 10^{-6}$	$< 10^{-6}$	$2 \cdot 10^{-4}$	$< 10^{-6}$	$5 \cdot 10^{-5}$	0.06	$2 \cdot 10^{-5}$	0.08
Aa	$< 10^{-6}$	$2 \cdot 10^{-5}$	$1 \cdot 10^{-3}$	0	<b>0.02</b>	$< 10^{-6}$	$2 \cdot 10^{-6}$	$4 \cdot 10^{-5}$	<b>0.02</b>	$< 10^{-6}$	0.39	<b>0.03</b>	$< 10^{-6}$	0.28	$5 \cdot 10^{-5}$
N	$< 10^{-6}$	$1 \cdot 10^{-3}$	$< 10^{-6}$	<b>0.02</b>	0	$2 \cdot 10^{-4}$	<b>0.01</b>	0.47	$7 \cdot 10^{-5}$	$5 \cdot 10^{-3}$	$8 \cdot 10^{-3}$	$< 10^{-6}$	0.13	0.18	0.31
Co	$< 10^{-6}$	$< 10^{-6}$	0.29	$< 10^{-6}$	$2 \cdot 10^{-4}$	0	$1 \cdot 10^{-4}$	$< 10^{-6}$	$< 10^{-6}$	$< 10^{-6}$	0.13	<b>0.02</b>	$< 10^{-6}$	$2 \cdot 10^{-4}$	$4 \cdot 10^{-6}$
Nu	$< 10^{-6}$	$8 \cdot 10^{-3}$	$2 \cdot 10^{-3}$	$2 \cdot 10^{-6}$	<b>0.01</b>	$1 \cdot 10^{-4}$	0	0.20	$5 \cdot 10^{-3}$	$3 \cdot 10^{-3}$	0.26	$3 \cdot 10^{-3}$	0.17	$8 \cdot 10^{-3}$	$9 \cdot 10^{-5}$
Ca	0.05	$< 10^{-6}$	$< 10^{-6}$	$4 \cdot 10^{-5}$	0.47	$< 10^{-6}$	0.20	0	$< 10^{-6}$	$< 10^{-6}$	$< 10^{-6}$	0.30	$< 10^{-6}$	$8 \cdot 10^{-4}$	$7 \cdot 10^{-6}$
Li	<b>0.01</b>	$< 10^{-6}$	$< 10^{-6}$	<b>0.02</b>	$7 \cdot 10^{-5}$	$< 10^{-6}$	$5 \cdot 10^{-3}$	$< 10^{-6}$	0	$< 10^{-6}$	$3 \cdot 10^{-5}$	$< 10^{-6}$	0.06	$3 \cdot 10^{-4}$	$2 \cdot 10^{-6}$
Ps	$4 \cdot 10^{-5}$	$< 10^{-6}$	$2 \cdot 10^{-4}$	$< 10^{-6}$	$5 \cdot 10^{-3}$	$< 10^{-6}$	$3 \cdot 10^{-3}$	$< 10^{-6}$	$< 10^{-6}$	0	$5 \cdot 10^{-4}$	0.07	$< 10^{-6}$	$6 \cdot 10^{-3}$	<b>0.03</b>
Ce	0.26	$3 \cdot 10^{-4}$	$< 10^{-6}$	0.39	$8 \cdot 10^{-3}$	0.13	0.26	$< 10^{-6}$	$3 \cdot 10^{-5}$	$5 \cdot 10^{-4}$	0	0.50	0.38	$< 10^{-6}$	$< 10^{-6}$
2M	$< 10^{-6}$	$1 \cdot 10^{-6}$	$5 \cdot 10^{-5}$	<b>0.03</b>	$< 10^{-6}$	<b>0.02</b>	$3 \cdot 10^{-3}$	0.30	$< 10^{-6}$	0.07	0.50	0	$8 \cdot 10^{-4}$	$< 10^{-6}$	<b>0.01</b>
Rx	$< 10^{-6}$	$< 10^{-6}$	0.06	$< 10^{-6}$	0.13	$< 10^{-6}$	0.17	$< 10^{-6}$	0.06	$< 10^{-6}$	0.38	$8 \cdot 10^{-4}$	0	$3 \cdot 10^{-3}$	$4 \cdot 10^{-5}$
Tr	$4 \cdot 10^{-3}$	$7 \cdot 10^{-3}$	$2 \cdot 10^{-5}$	0.28	0.18	$2 \cdot 10^{-4}$	$8 \cdot 10^{-4}$	$8 \cdot 10^{-4}$	$3 \cdot 10^{-4}$	$6 \cdot 10^{-3}$	$< 10^{-6}$	$< 10^{-6}$	$3 \cdot 10^{-3}$	0	$1 \cdot 10^{-6}$
Ot	0.46	0.08	0.08	$5 \cdot 10^{-5}$	0.31	$4 \cdot 10^{-6}$	$9 \cdot 10^{-5}$	$7 \cdot 10^{-6}$	$2 \cdot 10^{-6}$	<b>0.03</b>	$< 10^{-6}$	0.01	$4 \cdot 10^{-5}$	$1 \cdot 10^{-6}$	0

P-values of the Pearson's correlation coefficients between the populations of 24 different metabolic functional categories from the SUPERFAMILY database for 753 bacteria (the most significant values are in boldface). Correlations are calculated from fluctuations of categories from the average trend (see Methods). The (anti-)correlation is statistically significant for the most of the metabolic categories. We used the following short forms for the metabolic functional categories: En = Energy p/c, e- = Electrons transfer, Ph = Photosynthesis, Aa = Amino acids m/tr, N = Nitrogen m/tr, Co = Coenzyme m/tr, Nu = Nucleotide m/tr, Ca = Carbohydrate m/tr, Li = Lipid m/tr, Ps = Polysaccharide m/tr, Ce = Cell envelope m/tr, 2M = Secondary metabolism, Rx = Redox, Tr = Transferases, Ot = Other enzymes. Where m/tr stands for "metabolism and transportation" and p/c means "production and conversion".